TÉCNICO LISBOA

Multiobjective optimization of the energy storage systems (CHP and batteries) for small and new buildings

João Pedro Almeida Carneiro de Melo

Thesis to obtain the Master of Science Degree in

Energy Engineering and Management

Supervisor(s): Prof. Paulo José da Costa Branco

Examination Committee

Chairperson: Prof. Duarte de Mesquita e Sousa
Supervisor: Prof. Paulo José da Costa Branco
Member of the Committee: Prof. Carlos Augusto Santos Silva

October 2019

Acknowledgments

I would like to express my appreciation for everyone that, somehow, played a role in the development of this thesis.

I would like to thank my supervisor, Prof. Paulo Branco for all the help and guidance in the developing process of this thesis.

I also would like to say a big thank you to my parents for all their uncanny moral and financial support throughout my entire education. They helped me to keep my motivation and keep fighting for this Master Degree. Also, a big thank you to the rest of my family (my uncles, my grandparents and my cousins) for their support in this journey.

My girlfriend, Jessica, who was the one that was most present in the entire process of developing this thesis, who was responsible for motivating me every day and pushing me, a big thank you for being my rock.

My colleagues for this Masters, Manuel and Ricardo, a big thank you, this course without you guys would not be the same. We thrived and improved with all the unimaginable efforts in our projects.

To my friends, who supported me even if I was sometimes absent. They understood that this responsibility was my priority. Thank you.

Finally, I would like to thank every one from the electrical machines laboratory at Instituto Superior Técnico, for the advices and helpful comments that allowed me to improve my work.

For you all,

Thank you.

Resumo

Preocupações ambientais como o aquecimento global e a escassez de recursos, estão a levar ao desenvolvimento de novos sistemas de energia mais eficientes onde o consumo é maioritariamente satisfeito com unidades de produção própria. Estas unidades começaram a ser implementadas no sector residencial e comercial, para se obterem poupanças na fatura da eletricidade e para sensibilização ambiental. No mercado residencial, começaram a ser construídas as primeiras casas desligadas da rede, 100 % autossustentáveis, com um sistema de produção de energia baseado em fontes renováveis. No entanto, sistemas como este são mais difíceis de conceber para edifícios.

O trabalho desenvolvido nesta dissertação, analisou, melhorou e aprofundou um modelo previamente concebido que considerava o sistema de energia de um edifício residencial desligado da rede em Lisboa. Foram consideradas as tecnologias fotovoltaica e cogeração, a última, usada apenas em caso de emergência. Os perfis de produção e consumo deste sistema foram analisados. Por fim, foi feita uma avaliação económica e uma análise de sensibilidade aos resultados obtidos.

Foi concluído que o sistema fotovoltaico não conseguia satisfazer a totalidade do consumo, necessitando assim do uso de cogeração. O preço de eletricidade obtido com este sistema é mais alto do que o preço de venda de energia no mercado português. O decréscimo obtido na análise de sensibilidade não foi suficiente para o preço se tornar mais competitivo com o mercado.

Foram discutidas soluções para desenvolvimento futuro bem como considerações de pesquisa por forma a melhorar os resultados obtidos.

Palavras-chave: Fotovoltaico, Cogeração, Armazenamento de Energia, Edifícios autossustentáveis, Desligado da rede

Abstract

Environmental concerns about global warming and resource depletion are leading to new and more efficient energy systems, where the consumption of electricity is mainly satisfied with self-production units. Both the residential sector and the commercial sector started to integrate self-generation units in order to achieve cost-savings in electricity bills or to spread environmental awareness. The first off-grid and entirely self-sustainable houses also started to be built in the residential market. These houses have a production system based on renewable energies. However, this is more difficult to design for buildings.

The work developed in this thesis, analyzed a previously built model that considered the energy system of a residential building. Moreover, it aims to improve and provide deeper knowledge on off-grid residential buildings with the development of a new model. Photovoltaic and cogeneration (as an emergency source) technologies were integrated and the production and consumption profiles were analyzed. Finally, an economic assessment of the work was performed, as well as a sensitivity analysis.

It was concluded that the photovoltaic system could not operate on its own, requiring the use of cogeneration. The system with both technologies was more expensive than the utility companies' electricity price. The lower price obtained in the sensitivity analysis was not enough to be competitive with the utility companies' price.

Solutions for future developments and deeper research consideration were discussed in order to improve the results of this work.

Keywords: Photovoltaic, Off-grid, Energy storage, Self-sustainable buildings, Cogeneration

Contents

List of Tables

List of Figures

List of Acronyms

CHP Combined Heat and Power Plant.

DOD Depth of discharge.

LVN Low Voltage Network.

MPP Maximum Power Point.

MPPT Maximum Power Point Tracker.

PV Photovoltaic.

RMS Root Mean Square.

SOC State of Charge.

STC Standard Test Conditions.

List of Symbols

$Cons_{naturalgas}$ Natural gas consumption of the micro CHP.

E_j Total energy generated in year j.

G Solar irradiance.

I Current.

I_t Total investment cost.

I_{PV} Output current of the PV string.

I_{rms} AC current (Root Mean Square value).

$LCOE$ Levelized Cost of Energy.

$LCOE_{CHP}$ Levelized Cost of Energy for the micro CHP.

$LCOE_{PV}$ Levelized Cost of Energy for the PV system.

$LCOE_{System}$ Levelized Cost of Energy for the Energy System.

$NOCT$ Normal operating condition's temperature.

P Power.

$P_{J_{AC}}$ AC Joule power losses.

$P_{J_{DC}}$ DC Joule power losses.

$P_{J_{cables}}$ Total Joule power losses in cables.

$P_{\%losses}$ Power losses in percentage.

P_{load} Power needs of the building.

$Prod_{CHP}$ Electricity generated by the micro CHP.

R_{eq} Equivalent resistance.

S Cross-sectional area of a cable.

T_a Ambient temperature.

T_c Cell's temperature.

U Operating Voltage.

V_{DC} DC voltage.

$\eta_{Elec_{CHP}}$ Electrical efficiency of the micro CHP.

γ relative decrease in module efficiency per degree centigrade of cell temperature increase.

ρ Resistivity of copper.

a Discount rate.

$c_{fuel,j}$ Fuel costs of year j.

$c_{om,j}$ Operation and maintenance costs of year j.

$cos\varphi$ Power factor.

l Length of the cable.

n Lifetime of the energy system.

€ Euro.

Chapter 1

Introduction

1.1 Motivation

In 2016, 19.1 % of the total energy use for heating and cooling in the EU-28, was renewable energy. This reflects a significant increase of almost 9 percentage points from the value in 2004. What contributed to this growth was the increase use in the industrial, services and residential sectors [1].

The electricity consumption per unit of GDP is influenced by the energy efficiency of buildings. Moreover, the construction activity is the second highest contribution to the gross value added of the environmental economy. In this activity, the construction of passive buildings, buildings with low energy consumption and the renovation of existing buildings are included [1].

In Portugal, the residential sector has the third highest share of final energy consumption, with a share of 17%, after the transport sector with 37 % and the industry sector with 31 % [2].

An increase of 9.3 % in the electricity consumption of the residential consumer was registered in 2016 [2], related to the previous year. Moreover, in this year, the building sector led the electricity consumption with a share of 60.3 %, where the residential sector had a weight of 27.7 %. In this sector, the electric energy consumption represented 43.6 % followed by a renewable energy consumption with a share of 31.2 % [2].

The renewable energy produced within the EU-28 increased by 64 % between 2007 and 2017. Solar energy, although remaining with relatively low production, had a rapid expansion and represented a 6.4 % share of the renewable energy produced in 2017. The electricity generated from renewable sources increased during the period of 2007 to 2017, this growth "*reflects an expansion in three renewable energy sources across the EU, principally wind power, but also solar power and solid bio-fuels*" [3].

Knowing the weight of the residential sector in the Portuguese energy market and the European trend in the use of renewable energies in the production of electricity, as well as the implementation of renewable energies use in buildings, it is interesting to idealize a fully independent and off-grid building with a maximized generation from renewable sources.

1.2 Objectives

The scope of this thesis aims to build and analyze a model for the energy system of an off-grid building that generates electricity with renewable energies. The focal point is to assess a previously built energy system with *Photovoltaic* (PV) technology and provide improvements and deeper understanding on the energetic performance and consumption behavior of such building.

When it is proved that the renewable production is not enough, the off-grid building model will have a micro combined heat and power generator to work as an emergency source. Thus, the building would not be entirely off-grid, as it would be connected to the natural gas network, but it would still be electrically independent.

As a final task, the objective is to analyze the economic characteristics of the model built and perform a sensitivity analysis to assess if it is possible to decrease the system's costs.

1.3 Thesis Outline

This thesis studies and proposes improvements on methodology used and provide a deeper understanding about the use of PV technology for energy independent buildings. The data used such as weather data and building's specifications are the same used by Ladeira in his work [4], as well as some components of the energy system such as PV panels. In a first approach, some adjustments to the computation algorithm will be made. Inverter system will be included, as well as the power cables, in order to assess the importance of its power losses. After assessing the importance of power losses, the consumption profile will be analyzed and adjusted. The system will be re-designed for the new consumption profile and all new devices. The system's performance without batteries will be discussed. Batteries will be chosen to use in the system and the system's performance with batteries will be discussed. A micro combined heat and power plant will be implemented in the energy system as an emergency source of energy and finally, an economic assessment of the entire energy system will be performed.

Chapter 2

Background: PV systems

Solar systems can be characterized as active and passive systems. The active solar systems are responsible for converting solar energy into other forms of energy such as electrical or thermal energy. The passive solar systems are responsible to use efficiently the solar energy available, for example, heating and conserving the heat in a building through constructive strategies [5]. PV technology is an active solar system, it is based in the photoelectric effect, which is described by converting photons into electrical energy through PV cells. A PV module is constituted by PV cells arranged in series and/or parallel. Most of solar PV technologies nowadays are crystalline silicon-based. Tests in laboratory showed that a silicon terrestrial PV module can reach an efficiency of 22.9 % at *Standard Test Conditions* (STC), conditions described by a temperature of 25 ^{o}C and a solar irradiance of 1000 W/m^2 [6]. Each cell can generate a *Direct Current* (DC) power of about 1.5 W (0.5 V and a 3 A) and the number of cells depends on the panel technology. The lifetime of a PV system, with the correct maintenance, is higher than 20 years, making this a very reliable source of renewable energy [7].

Between 2003 and 2014 the global installed capacity of PV grew at an average rate of 49 % per year. Decentralized systems represent the majority of the global market with a share of 60 % and the centralized ones, operate at utility-scale and represent a share of 40 %. Most applications are now on-grid systems, however, off-grid systems, that once dominated the market, still show developing potential for some applications, for example, helping to provide energy in remote areas without access, in developing countries [8].

The prices of PV systems tend to decrease as the investments in such systems expand. The investment in autonomous systems is divided by; investment in batteries which represent the largest share of the investment, greater than 40%; investment in PV panels that represent a share between 15-20% of the investment; the inverter, also with a 20% share; and the remaining costs for control systems and other costs. The price of an installation depends on the location, the size of the system and components that need to adapt the consumer's needs, thus, it is difficult to define [7].

2.1 PV systems types

Regarding its electric network connectivity, a PV system can be classified in two types: grid-tied and autonomous systems (or off-grid).

The hybrid systems with several energy sources (PV, diesel generators, wind, etc.) are considered a third type. Under the scope of this thesis it is important to describe this type of system, as it stated in section 1.2, the system will have a micro combined heat and power generator [7].

2.1.1 Grid-tied system

In grid-tied systems, the connection to the electric grid allows for load management solutions such as the net balance contracts and the sale of electricity contracts (with the power distribution companies). The generated energy is injected directly in the grid and accounted with the use of energy meters. Therefore, in this case, batteries and regulators are not necessary for the system to work, this simplifies the system and allows for low maintenance [7].

2.1.2 Off-grid system

The term autonomous or off-grid system is used because the system lacks any connection to the electrical grid. In an off-grid system that does not have energy storage, consumers use immediately the electric energy produced by the PV module. The investment in a system without energy storage is lower compared to systems with energy storage devices. However, consumers only have a supply of energy during energy production hours [7].

Off-grid PV systems with energy storage are constituted by a string of PV panels, an inverter, a controller to monitor and control the batteries' *State of Charge* (SOC) and a battery pack. The energy produced by the PV panels is supplied to the load, and the surplus energy is stored in the batteries. The stored energy can be used during low or non production hours, when there is low to none solar radiation. Hence, the batteries must have a capacity that allows to feed the load during such hours (typically during the night and in low solar radiation days). The controller has the ability to cut-off the PV production and also cut-off the consumers supply accordingly to the batteries' SOC. The inverter efficiency and consumption in stand-by reduces the amount of available power to the loads. The battery pack of the system can be either connected in series with the PV panels, controller and inverter or in parallel. On one hand, if the battery pack is connected in series, the inverter is connected to the battery, on the other hand, if the battery pack is connected in parallel, the inverter will be connected to the controller [7]. There are some applications of inverter with a charge controller integrated.

2.1.3 Hybrid system

Hybrid systems are systems that combine at least two energy sources for production (example: PV and cogeneration). The energy sources can be renewable or non renewable. There is a high degree of

complexity associated with these systems. The different energy sources and the unpredictable behavior of some of them are responsible for such complexity.

Alike PV systems, the hybrid system can be classified as grid-tied and off-grid system. Moreover, these systems can be also classified for its nominal power capacity, priority of energy source and configuration [9].

Nominal power capacity classification

The classification of hybrid systems by nominal power capacity is divided by categories as follows:

• Hybrid micro-system: With a nominal capacity lower than 1 kW, this system is mostly used to supply a single and small load;

• Low power hybrid system: With a nominal capacity between 1 kW and 100 kW, this is currently the most common types of system;

• Medium power hybrid system: Its capacity has a range between 100 kW and 1000 kW;

• High power hybrid system: Its capacity is higher than 1000 kW. This type of systems it's very uncommon [9].

Prioritized source of energy classification

Regarding the classification of the hybrid system by priority of energy source, it can be a hybrid system that mostly produces from a non renewable source or a hybrid system that mostly produces from a renewable source.

In system that mostly produces from a non renewable source the load would be primarily fed by the diesel generation unit. During periods of low consumption where the diesel unit has low efficiency due to a very small loads, the energy from renewable sources would be used to satisfy the consumption. Moreover, the energy from renewable sources could complement the energy generated by the diesel unit. The excess energy produced from renewable sources is stored in a battery pack for future utilization. In this type of systems, the energy from renewable source is lower than the average daily consumption.

In a system that mostly produces energy from renewable sources, the diesel generator operates only as a backup system. This generator only operates when the generation from renewable sources is low and the consumption is high. In this energy system, the production from renewable source must provide a significant contribution to supply the average daily load.

Hybrid systems are design to operate between the two mentioned extremes. It will always tend to one of the extremes depending on the characteristics of the location where it is installed. This will dictate their technical and economical viability [9].

Configuration classification

A hybrid system can be classified as in series, commuted or parallel. In this section, solar PV is the renewable energy considered and a diesel generator is the non renewable one, to use as an example.

• Hybrid system in series

The energy transport to the load is sequential. All the energy sources are used to charge the battery pack and the battery pack is used to supply the load;

• Commuted Hybrid system

In this situation, the battery pack can be charged by the diesel generator and/or by the PV panels. The load can be supplied by the diesel generator or by the PV panels, but not by both at the same time;

• Hybrid system in parallel

All sources can supply the load by syncing the inverter and the energy sources. Usually a bi-directional inverter is used to charge the battery pack or to act as an inverter when the battery pack is supplying energy to the load [9].

2.2 PV systems components

A PV system is basically composed by the following elements: a set of PV modules, responsible for the production of energy; batteries, responsible for the storing of the energy produced; a regulator, responsible to manage and control the SOC of the batteries; an inverter, responsible to convert from DC to *Alternating Current* (AC) and the load that represents the consumption of energy [7].

2.2.1 PV panel: working principle

The power output of a PV cell depends on the cell's temperature, T_c, and on solar irradiance, G, given in W/m^2, this is described in equation 2.1, combining with equation 2.2, that show the efficiency variation with cell's temperature. The efficiency of a cell decreases with an increase in temperature [5] [10].

$$P_{PV} = \eta(T) * A_{PV} * G \tag{2.1}$$

$$\eta(T) = \eta(STC)[1 + \gamma(T_c - 25^{\circ}C)] \tag{2.2}$$

Where, γ is defined as the relative decrease in module efficiency per degree centigrade of cell temperature increase [10].

The cell's temperature depend on the ambient temperature and on solar irradiance. Equation 2.3 specifies the cell's temperature, using the normal operating condition's temperature, $NOCT$, in °C, of the PV cell [10].

$$T_c = T_a + \frac{NOCT - 20}{800} \cdot G \tag{2.3}$$

Where T_a is the ambient temperature, $NOCT$ is the normal operation condition's temperature and G is the solar irradiance.

2.2.2 Inverter

Any isolated PV system , should have an off-grid inverter as this is an essential electronic device that converts low voltage DC electricity from a battery or other power source to 100 V - 120 V or 220 V - 240 V AC signal depending upon the need of the load. Off-grid Inverters produce a voltage wave, with an independent frequency from the grid. This type of inverter convert DC to AC power and it may also regulates the PV system if correctly sized according to the battery voltage levels. Some requirements are indispensable for an off-grid inverter [7].

- Auto starting and adequate protection warning signs;
- Peak power capacity – it should support more than two times its nominal power;
- Low stand-by power; High efficiency; Voltage stability – between the range of 230 V $\pm$ 10
- Possibility to connect other inverters in parallel.

Some inverters and *Maximum Power Point Trackers* (MPPTs) have controller functions integrated, these devices can operate as a regulator that manages and controls the SOC of the battery.

2.2.3 Battery

An electric battery is used to store energy, this device converts stored chemical energy into electrical energy in accordance to the chemical reactions of reduction and oxidation - redox equations. The primary cells were largely replaced by rechargeable batteries, due to resource savings and pollution reduction. The type of batteries that are more common for storing applications are lead-acid batteries, but these are being replaced by Lithium-ion batteries over time due to several advantages. The Li-ion batteries have high capacity, high electrochemical potential, superior energy density, superior durability, as well as the flexibility in design. All the properties above accelerate the substitution of conventional secondary batteries [7].

The batteries integrated in autonomous PV systems must have the following characteristics:

- Reduced maintenance requirements;
- Long service time;
- Reduced self-discharge and high energy efficiency;
- High storage capacity and power density;
- Good performance/price relation;
- Protection against the occurrence of hazards to the environment and health.

Chapter 3

Improvements in the PV system model

3.1 Initial system and considerations

The starting point for this thesis is based on a previous thesis developed by Ricardo Ladeira [4]. In his work, he studied and analyzed the energy needs in a small 9-apartment building, with 3 floors, as this is the most common type of building in downtown Lisbon, where it would be located. He considered that the building was not yet built, thus, it would be designed to integrate renewable energy technologies in its own self generation energy system and would be disconnected from the grid. The apartments were considered to be small T2's with 89 m^2 of area, they would have 2 bed rooms, a bathroom, a kitchen and a living room. The common area for stair and elevator was considered with 23 m^2, thus resulting in a building's floor area of 290 m^2. He also considered a flat roof, thus the total area of the roof was 290 m^2.

The energy system of this building was composed by a PV system, battery energy storage and a diesel generator. Ladeira's computations would relate the fluxes of energy between PV production, battery pack and consumer, as well as the assessment of using an emergency diesel generator. However, a PV system was designed with the simple consideration of producing the total amount of electricity necessary to satisfy, almost entirely, the energy consumption of all apartments. The operational design of the solar panels was not specified, the number of panels in series and in parallel was not addressed. The number of inverters and the number of strings per inverter were not addressed, the balance of the system was not yet taken into account. With these considerations, no current or voltage changes were assessed. The power generated by the PV system was computed based on weather data in Lisbon, such as the incident radiation and ambient temperature, and PV panel data such as the change of cell's efficiency with temperature. However, cell's temperature was considered as the same as ambient temperature, the thermal stability of the system was not addressed. The values measured for the ambient temperature in the Lisbon area (thus, cell temperature), are between -0.9 ºC and 40.48 ºC. The slope of the panels were considered with 35 º of slope, this consideration will be used for this thesis as well.

In such methodology, no power losses were considered. Some examples of power losses are joule losses in cables due to transport and losses due to inverter's efficiency and battery's efficiency.

During the power computations, no secondary devices that are necessary to the system were considered, such as inverters, MPPTs and charge controllers.

The battery pack was considered to be a hypothetical giant reservoir of energy installed in the building. This reservoir had properties of a Lithium Iron Phosphate ($LiFePO_4$) battery, such as specific energy, energy density, cycle life, energy efficiency and self-discharge. The battery's capacity and SOC was computed in different scenarios. The *Depth of discharge* (DOD) considered was 90 %. The battery's capacity was considered constant with its utilization and the amount of charge and discharge cycles was not assessed, thus, the loss of capacity with cycle life was not assessed.

The micro combined heat and power plant that Ladeira considered had a nominal power of 20 kW, it was a XRGI 20, from EC Power and was fueled by natural gas. This unit is ideal for small and medium sized residential buildings [4]. In his study, he determined that this generator had enough power to support the building's consumption needs. However, he did not consider the possibilities of using its heat supply. The electricity demand could be reduced. The rules for the generator operation set by Ladeira were, if the battery's SOC reaches 10%, the generator is turned ON, and it produces electric energy until the SOC reaches 90%. While operating, the generator prioritizes the consumption of the building, leaving the excess energy for charging the battery.

Ladeira's study analyzed several scenarios. These scenarios considered only the percentage of energy that was supplied with the PV system and the amount of roof area available to use.

3.2 Temperature effects

The estimation of the power produced by a solar cell considers the cell temperature and not the ambient one. Therefore, using equation 2.3 and the $NOCT$ given in the manufacturer datasheet in appendix A.1, 45 ºC, the cell's temperature was computed. It varies between -0.9 ºC and +70.29 ºC while the ambient temperature is the same as in section 3.1, between -0.9 ºC and 40.48 ºC. Note the almost 30 ºC of temperature difference during the summer. Figure 3.1 describes the cell's efficiency for the temperature range of the cell in the Lisbon area. The 30 ºC of temperature difference, reflect a difference in efficiency of 2.2 %.

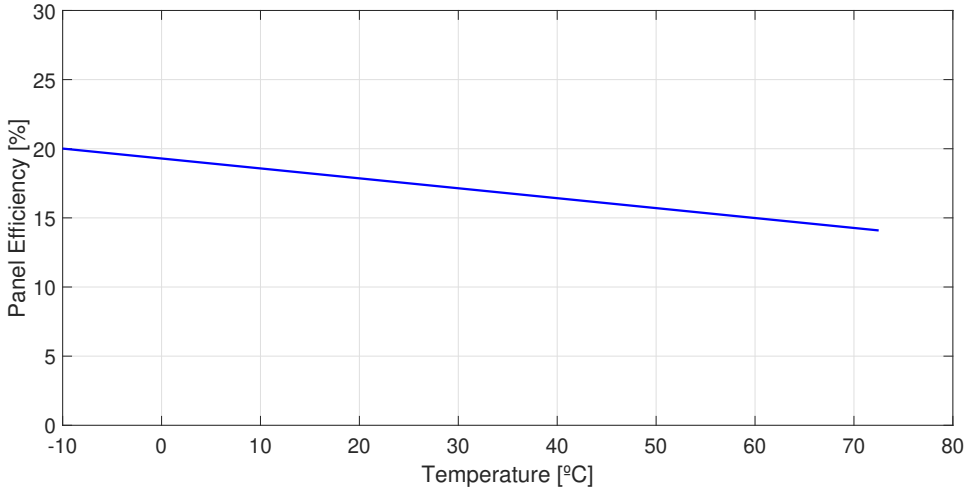

Figure 3.1: Variation of the cell's efficiency with temperature

3.3 Operation and topology of the photovoltaic system

A PV system is described as a set of strings with modules connected in series. All the modules must be connected to an inverter that converts from DC to AC. As a starting point, no charge controllers or batteries will be integrated in the system, this allows to assess the weight of the power cables' losses. The base case developed by Ladeira used to obtain the operational design of the system, was the one considering full roof coverage (around 60 % of the roof area covered with panels). The operational design obtained is described as 6 strings with 20 modules connected in series in each string.

The inverter chosen has a double input profile (2 MPPTs),with one string per MPPT, the system has 2 strings per inverter and a total of 3 inverters. Each inverter will supply energy to a specific floor. Each inverter has 3 output power cables, since every floor has 3 apartments, each output power cable of an inverter will transport energy to an apartment.

Figure 3.2 illustrates the described system. In this case, apartments 1, 2 and 3 would belong to floor 1, apartments 4, 5 and 6 would belong to floor 2 and apartments 7, 8 and 9 would belong to floor 3, this shows that one inverter supplies one floor.

The specifications of the PV system and inverter are described in table 3.1, the PV system operates with a voltage close to the nominal voltage of the inverter (620 V), it has a total of 36 kWp of peak power and an *Maximum Power Point* (MPP) operating voltage of 634 V. The compatibility of the PV system with the inverter was analyzed and assured. The open circuit voltage of each string (778 V) is lower than the maximum DC input voltage of the inverter (1000 V). The configuration per MPPT is balanced, each MPPT is connected to the same number of panels. The MPP voltage of the system (634 V) is within the range of operation of the inverter (440-800 V). The DC power per MPPT (6 kW) is lower than the DC power limitation per MPPT (12 kW). The MPP current per MPPT (9.47 A) is lower than the maximum DC input current per MPPT (25.0 A), and the total input current of the inverter (summing the MPP current of 2 MPPTs, 18.94 A) is lower than the maximum DC input current of the inverter (50.0 A). The input short circuit current per MPPT (10.07 A) is lower than the maximum input short circuit current for each

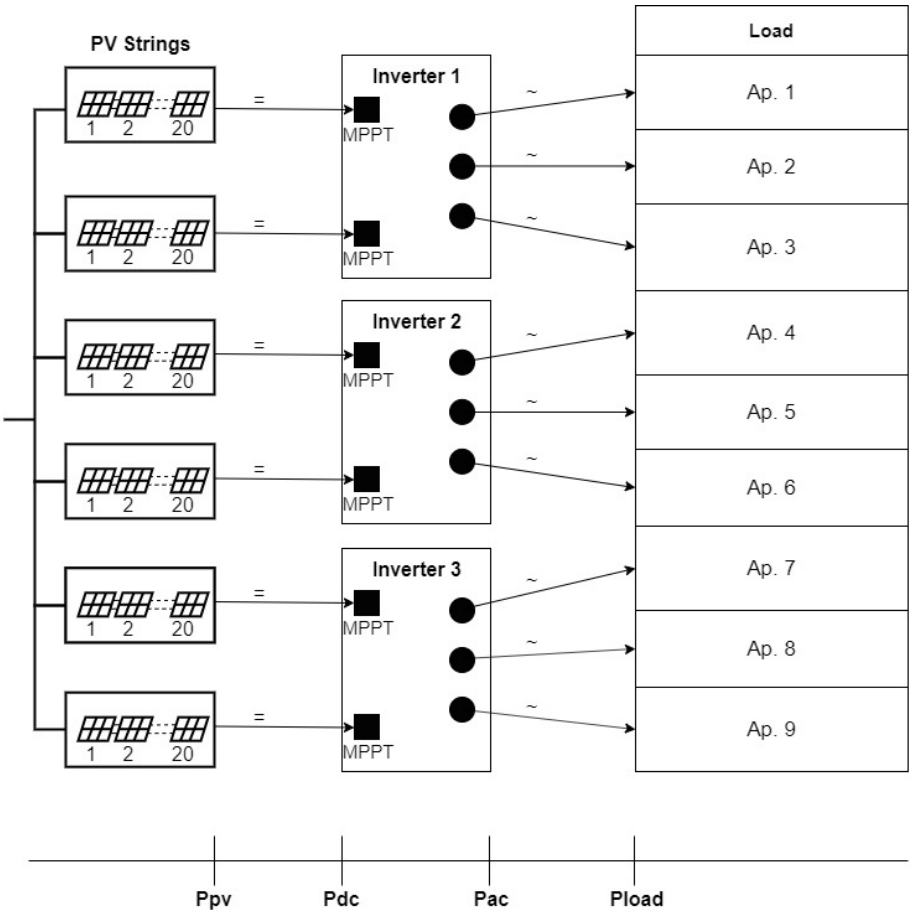

Figure 3.2: Electricity flow from generation to load

MPPT (30.0 A). This analysis assures that the PV system is indeed compatible with the model of inverter chosen.

With the energy system compatible and ready to connect, one needs to size the power cables that transport energy from the PV system to the grid in order to be able to estimate the power cables' losses.

PV System		Inverter	
Peak Power [kW]	36	Maximum DC Input Voltage [V]	1000
MPP Voltage [V]	634	DC input voltage range with parallel configuration of MPPT at rated AC Power [V]	440...800
MPP Current [A]	9.47	DC power limitation for each MPPT with independent configuration of MPPT at rated AC Power, max unbalance example	12000 W [480V <=V_{MPPT}<=800V] the other channel: P_{DCr}-12000W [350V <=V_{MPPT}<=800V]
Open Circuit Voltage [V]	778	Maximum DC input current ($I_{DC_{max}}$) / for each MPPT ($I_{MPPT_{max}}$) [A]	50.0 /25.0
Short Circuit Current [A]	10.07	Maximum input short circuit current for each MPPT [A]	30.0
MPP Power per String [kW]	6	Rated DC input voltage [V]	620
Brand of the module	LG	Number of independent MPPT	2
Model of the module	LG300S1C-A5	Rated DC input Power [W]	20750
		Brand	ABB string inverters
		Model	TRIO-20.0-TL-OUTD
		Weighted efficiency (EURO)	98 %

Table 3.1: Specifications of the PV system and inverter

3.4 Sizing the power cables

The power cables connect all the components of the system, from figure 3.2, direct current flows in the power cables that connect the PV strings to the inverters and alternate current flows in the power cables that connect the inverters to the apartments. In this first approach, the system has PV modules on top of the building (roof), connected to inverters (placed on the ground next to the building) connected to the apartments (load), has it is observed in figure 3.3. One must consider that the DC side of the inverter has one cable per MPPT and the AC side, as it is a three-phase inverter with one cable per phase, has three cables. Thus, and with figures 3.2 and 3.3, direct current flows in six power cables and alternate current flows in nine power cables. In figure 3.3, the DC power cables are numbered from 1 to 6 and the AC power cables are numbered from 9 to 15.

Using figure 3.3 to identify the cables, the length estimated for each cable is given in table 3.2

Now, one must estimate the section of the DC power cables, the MPP output current from the PV system is 9.47 A and the short circuit current is 10.07 A. Using table A.3 from the Low Voltage Catalogue of Grupo Cabelte, one can obtain a section of 1.5 mm^2. The maximum admissible current for this cable is 15.5 A.

To estimate the section of the power cables in the AC side, it's necessary to compute the *Root Mean Square* (RMS) value of the current. The computational method described in section 3.5, shows how the RMS value for the current is obtained and estimates the cable's power losses.

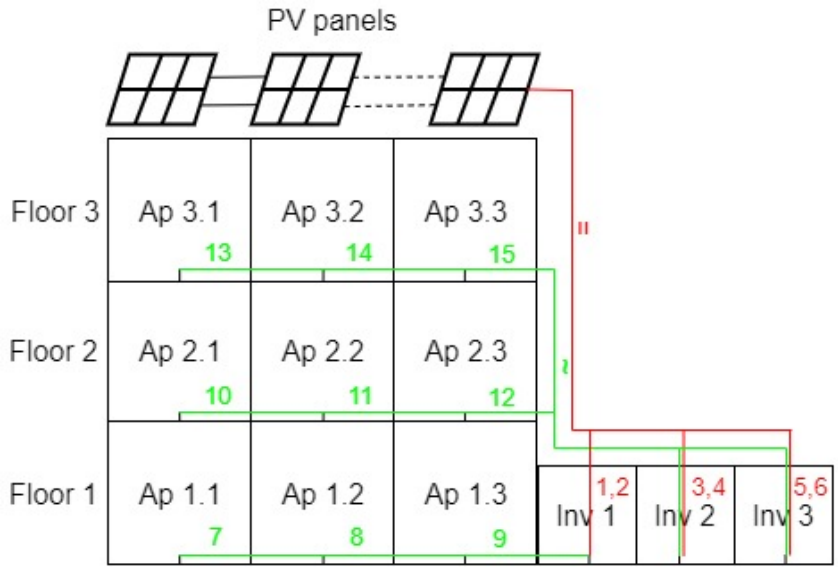

Figure 3.3: Scheme of the power cables connections in the building

DC side		AC side	
Cable number	Estimated length [m]	Cable number	Estimated length [m]
1 and 2	102	7	131
3 and 4	103	8	81
5 and 6	104	9	31
		10	139
		11	89
		12	39
		13	147
		14	97
		15	47

Table 3.2: Length estimation for the power cables

3.5 Estimating power cable's losses

With the geometry of the cables estimated, is now possible to compute the power losses in cables, one considered the cables as an equivalent resistance, R_{eq}, with equation 3.1 and computed the total Joule power losses, $P_{J_{cables}}$ with equation 3.4. The Joule losses in the DC side were computed with equation 3.2 and on the AC side with equation 3.3.

$$R_{eq} = \frac{\rho \cdot l}{S} \tag{3.1}$$

$$P_{J_{DC}} = R_{eq} \cdot I^2 \tag{3.2}$$

$$P_{J_{AC}} = R_{eq} \cdot I_{rms}^2 \tag{3.3}$$

$$P_{J_{cables}} = P_{J_{DC}} + P_{J_{AC}} \tag{3.4}$$

where ρ is the resistivity for copper, l the length of the cable, S the cross-sectional area and I is the current that flows in that cable. The sum of all the losses in cables represents the total cable losses of the entire energy system. Note that $P_{J_{DC}}$ represent the DC Joule power losses in cables connecting the PV strings and the inverter, and that $P_{J_{AC}}$ represent the AC power losses in cables connecting the inverter and the load (see figure 3.2).

The current must be computed using equation 3.5.

$$P = U \cdot I \tag{3.5}$$

where P represents the power, U the operating voltage and I the current. Thus, the current for the PV strings, I_{PV} is computed with equation 3.6.

$$I_{PV} = \frac{P_{PV}}{U_{PV}} \tag{3.6}$$

Then, the DC power losses were calculated using equation 3.2 for each cable, where $I = I_{PV}$ and R_{eq} is the electric resistance of each cable. The sum of the losses in each cable results in the DC power losses. Afterwards, using equation 3.7, the DC power was computed, this is the power at the input of the inverter as shown in figure 3.2.

$$P_{DC} = P_{PV} - P_{J_{DC}} \tag{3.7}$$

Considering the inverter's efficiency, the AC power at its output was computed using equation 3.8.

$$P_{AC} = P_{DC} \cdot \eta_{inv} \tag{3.8}$$

The AC current, I_{rms}, was obtained with equation 3.9 to compute the AC power losses and to obtain the section of the power cables in the AC side. $cos\varphi$ represents the power factor.

$$I_{rms} = \frac{P_{AC}}{3 \cdot U_{phase} \cdot cos\varphi} \tag{3.9}$$

The AC power losses were computed for each cable using equation 3.3 and then, the sum of the losses in each one of the nine cables resulted in the total AC power losses.

The net power that the load receives from the PV system becomes established using equation 3.10, this is the power at the input of the load as observed in figure 3.2.

$$P_{load} = P_{AC} - P_{J_{AC}} \tag{3.10}$$

Figure 3.2 is a scheme that describes the different stages of power computations along the electricity flow, from generation to load, as well as the system operational design.

3.5.1 Results and discussion

The methodology described in section 3.5 was used to obtain the cross-section of the power cables in the AC side and to assess the power losses in cables for the coldest day of the year (to ensure thermal comfort the load increases). The power losses in cables were computed to evaluate it's importance in the energy system. Note that the PV power used to assess such losses is the hourly average power during production hours of the coldest day, this is shown in figure 3.4. For the coldest day, production started at 10:00 and ended at 19:00, the average production of power during this period was 12240.9 W.

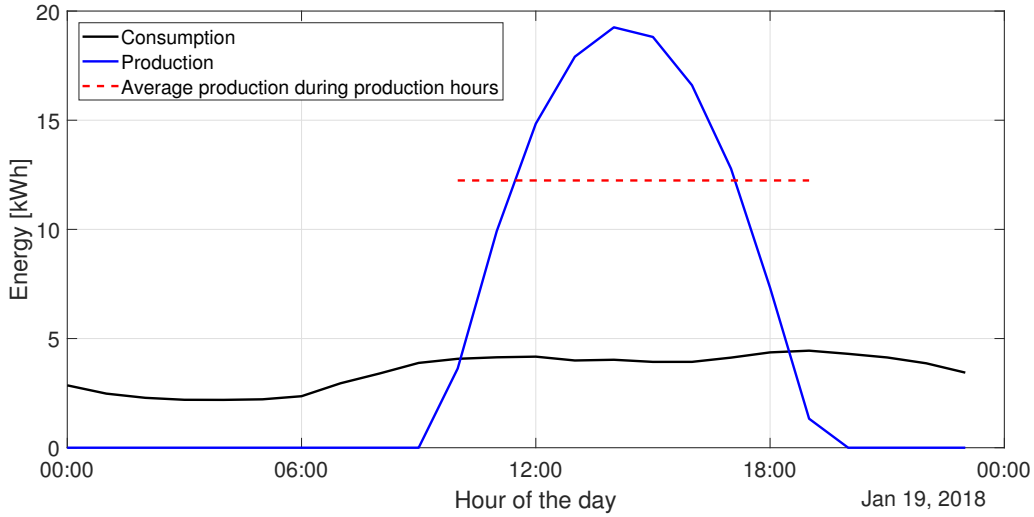

Figure 3.4: Hourly energy consumption, production and average production during production hours for the coldest day of the year

The results for power computed in several stages of the system are given by:

$P_{PV} = 12240.9$ W

$P_{DC} = 12172.6$ W

$P_{AC} = 11929.2$ W

$I_{rms} = 7.2$ A

$P_{load} = 11394.0$ W

The section of the power cables in the AC side was obtained using the table from appendix A.3, since

$I_{rms} = 7.2$ A the cable's section is 1.5 mm^2 and the maximum admissible current is 15.5 A.

The total power losses in the cables have a value of $P_{J_{cables}} = 603.5$ W which can be related to the generation as a percentage lost: $P_{\%losses} = 4.9$%.

The power losses obtained were evaluated specifically for the system described in section 3.3, if the system's design change, the influence of cable losses may change as well.

Chapter 4

Residential sector: energy consumption profile

Data on the energy consumption profile for the residential sector was obtained from the Update of the Consumption, Production and Self-consumption for the Year of 2019: Methodological Document, of EDP: Distribuição [11], which is the utility company responsible for the distribution of electric energy in the Portuguese grid. In this document, the profiles are obtained considering an average of the population that are inserted in a certain consuming group. The profile is a hourly average of energy consumed, normalized to sum 1000 units in a year, so, the hourly values represent a permillage of the total energy consumed in a certain year. Although the document addresses the adjustment of profiles for 2019, the last annual average consumption known is from 2017. Hence, for the purpose of this work, the values obtained for hourly consumption along the year were obtained by considering the permillage obtained in the profile estimation and the total energy consumed by the residential sector class in 2017. Table 4.1 describes the different profiles for the *Low Voltage Network* (LVN), in Portuguese, *Baixa Tensão Normal*, BTN.

	Profile		
	LVN A	LVN B	LVN C
Power [kVA]	$>$ 13.8	$\leq$ 13.8	$\leq$ 13.8
Annual consumption [kWh]	Any annual consumption	$>$ 7140	$\leq$ 7140
Average annual consumption in 2017 [kWh]	13 224	11 696	1681

Table 4.1: LVN profiles from EDP report [11]

The residential sector's consumption is well represented by the LVN, class C profile. Customers that are inserted in this profile have an annual consumption lower or equal to 7140 kWh and a power lower or equal to 13.8 kVA. The average annual consumption of the LVN C profile in 2017 was 1681 kWh. The profile developed by EDP was based on 15 minutes samples. However, for the purpose of this work, the profile was adjusted to consider an hourly base of energy consumption, simply summing each

4 values of 15 minutes. Consumption profile LVN class C is similar for different days of the week and during the weekend. However, it has a large variation depending on the seasons. During Winter months, the consumption increases. Figures 4.1, 4.2 and 4.3 describe the average consumption for the LVN C profile, during different days and for different months of the year. In such figures, it is possible to observe that for winter months the consumption of energy is higher.

4.1 Week and weekend analysis

In figure 4.1, for a typical week day, the lowest consumption is achieved between 04:00 and 06:00. The consumption then increases until 08:00 and follows a stable trend to increase slowly between 08:00 and 13:00. At 13:00 the consumption reaches a local maximum and decreases slowly until around 16:00/17:00. Afterwards, the consumption increases until around 21:00 where it reaches its' daily maximum, a higher consumption of energy occur around dinner time between 20:00 and 22:00. Finally, the energy consumption decreases until mid night.

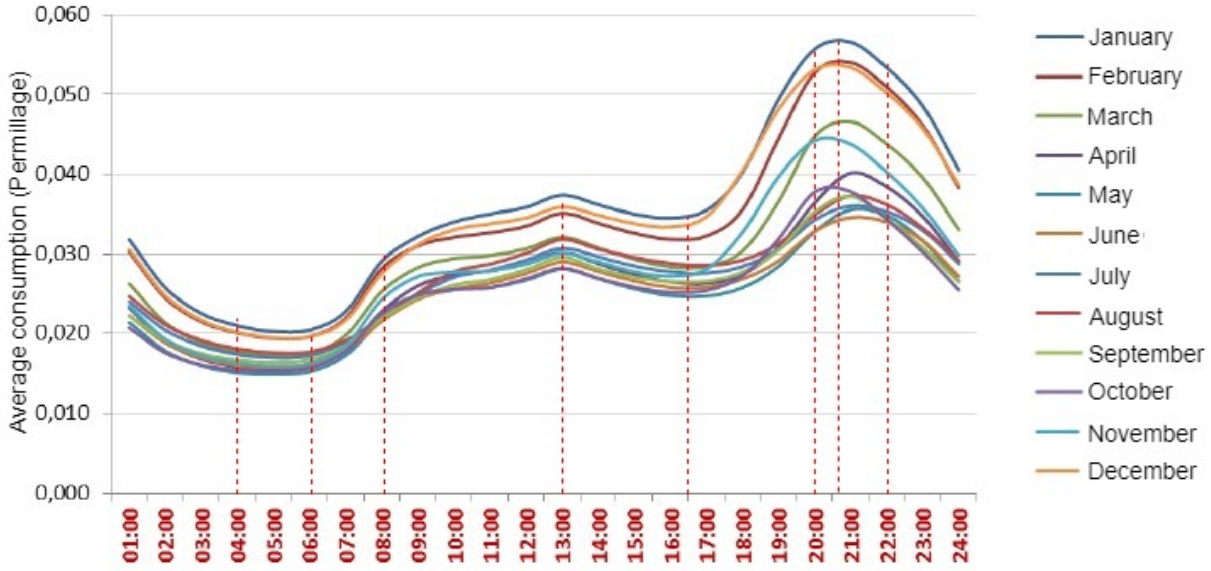

Figure 4.1: Average consumption profile for a typical week day per month (January to December) of LVN class C [11]

For Saturdays' profile, observed in figure 4.2, the energy consumption is very similar to the profile for week days, with the consumption being higher during the entire day except during the period of 08:00 to 09:00. The maximum daily consumption is also observed at dinner time (20:00/21:00). The minimum daily consumption is observed between 04:00 and 06:00. The local peak of consumption at lunch time is higher during Saturdays when compared to week days, as expected.

For Sundays, the profile observed in figure 4.3 is very similar to Saturdays' profile. There is a slight difference for the lunch period (between noon and 14:00), since this period has an increased weight than observed for Saturdays. The maximum daily consumption is around dinner time (20:00/21:00) and the minimum is between 05:00 to 07:00.

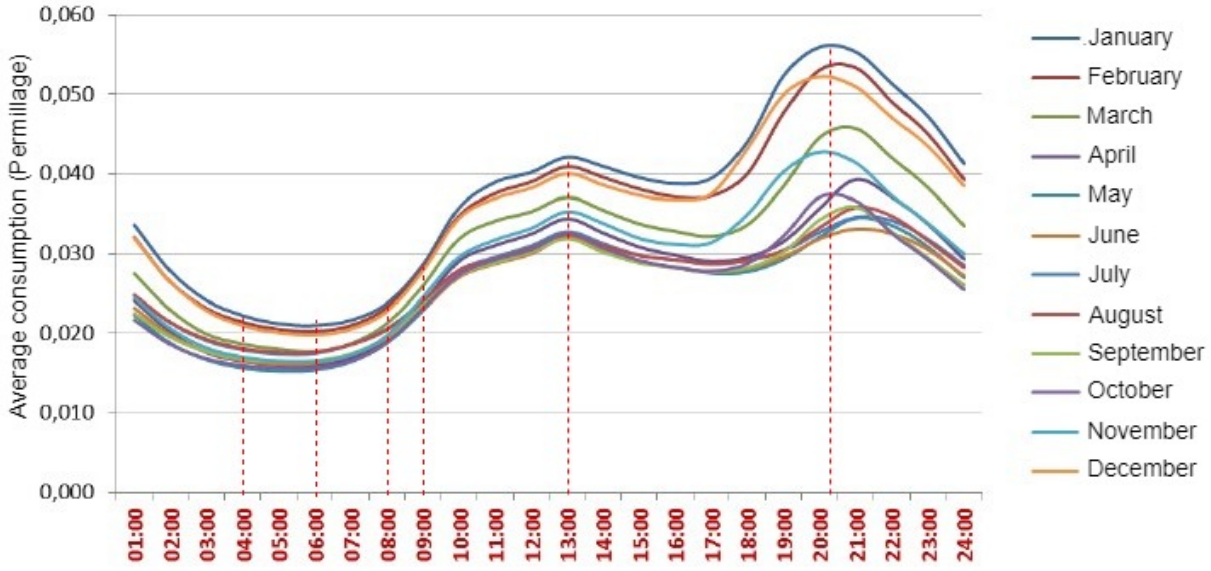

Figure 4.2: Average consumption profile for a typical Saturday per month (January to December) of LVN class C [11]

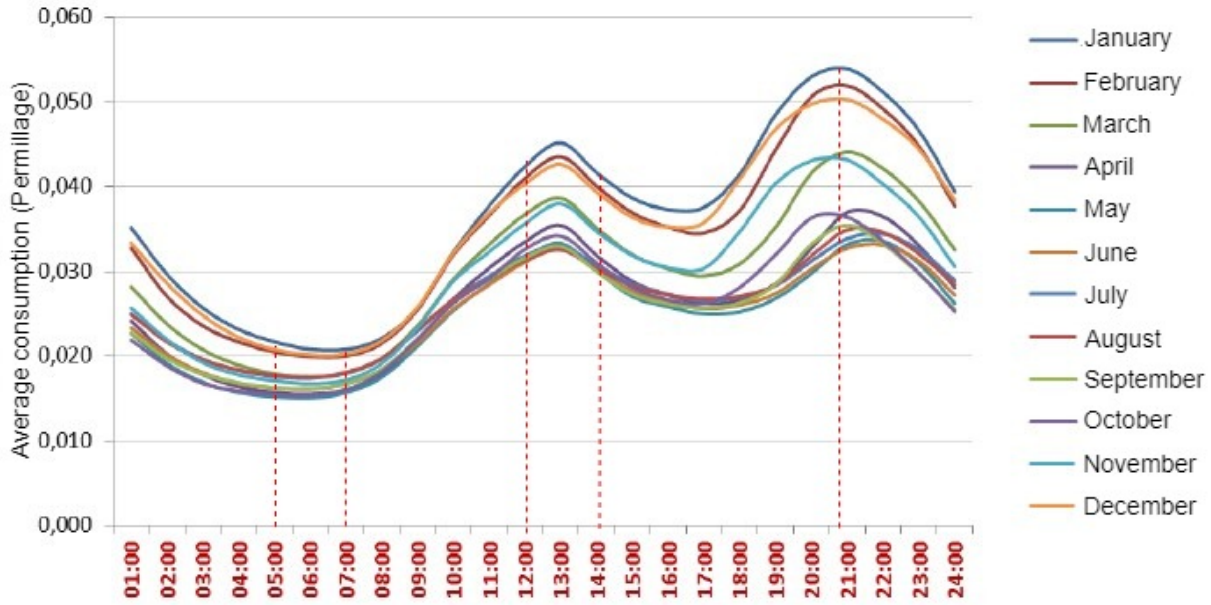

Figure 4.3: Average consumption profile for a typical Sunday per month (January to December) of LVN class C [11]

Chapter 5

PV system

The PV system needs to be tested for the new consumption profile. The testing phase has two steps, first the system is tested without batteries, and afterwards with batteries already implemented. However, with the change of the consumption profile to a residential sector specific profile, the system must be reviewed. Since the profile of consumption decreased, the power required is now lower, thus, the system does not require to have as much PV panels as before. Since the decrease in consumption was around 60%, the system will have a decrease in peak power. This decrease will not be lower than 60% and the balance of the system will be ensured.

5.1 Re-sizing the PV system

The new operation of the PV system was designed considering that batteries will be implemented further into the work. Since batteries are being considered, a device that controls the battery's charge must be included in the system. There is a type of inverter that is also a charge controller to the battery, and a type of MPPT that also has charge controller functions, thus, both of this devices, the inverter charger and the MPPT charge controller, have the necessary requirements to be integrated in the system.

The previous peak power of the system was 36 kWp, with the decrease of 60% in the consumption profile assumed, the peak power for the new system will decrease but will not be lower than 21.6 kWp. While choosing the configuration of the system and the devices used, it was necessary to consider the voltage and output current of the PV panels, the max input current and operating voltage of the inverter charger, the max solar power recommended and the operating voltage of the MPPT charge controller and the max charging current of the battery and its operational voltage. The compatibility of both the inverter and MPPT charge controller with battery's operational voltage had to be ensured.

The final design was obtained considering all these parameters that influence the assembly of the system. The system has a configuration that is equal for every floor, because at this stage the consumption for all apartments is being considered as equal to the average consumption of the LVN C profile described in chapter 4, with this consideration it is easier to account for weight distribution in all floors

and there is an ease of access to the batteries for maintenance. This floor configuration is described as a set of 5 strings in parallel with 2 panels in series is connected to every MPPT charge controller that connects to an inverter and a set of 2 strings in parallel with 2 panels in series is connected to every MPPT charge controller that connects to a battery pack. Each floor will have 20 panels connected to 2 MPPT charge controllers that connects to an inverter charger and 4 panels connected to 1 MPPT charge controller that connects to a battery pack and a battery pack with 3 modules, the choice of the battery, as well as the assessment of system requirements for the battery pack will be discussed in section 5.5. Figure 5.1 illustrates the described scheme, in this figure, the arrows represent the power cables and the flow of electricity. In this design the key aspect to consider was not the power delivered to the load but rather the amount of energy available during the entire day. The coldest day of the year was verified as one of the days with the highest consumption. The objective designing the system was to ensure that the total production during the coldest day would be higher than the total consumption during this same day, allowing to charge the batteries and always ensuring that the system was balanced. The coldest day of the year is the most day important to assess that the energy needs are met, this is because during this day the inhabitants of the apartments consume more electricity than usual in order to ensure thermal comfort. Since this thesis discusses the energy system of a residential building, one must consider the needs and comfort of it's users and thermal comfort is essential for people.

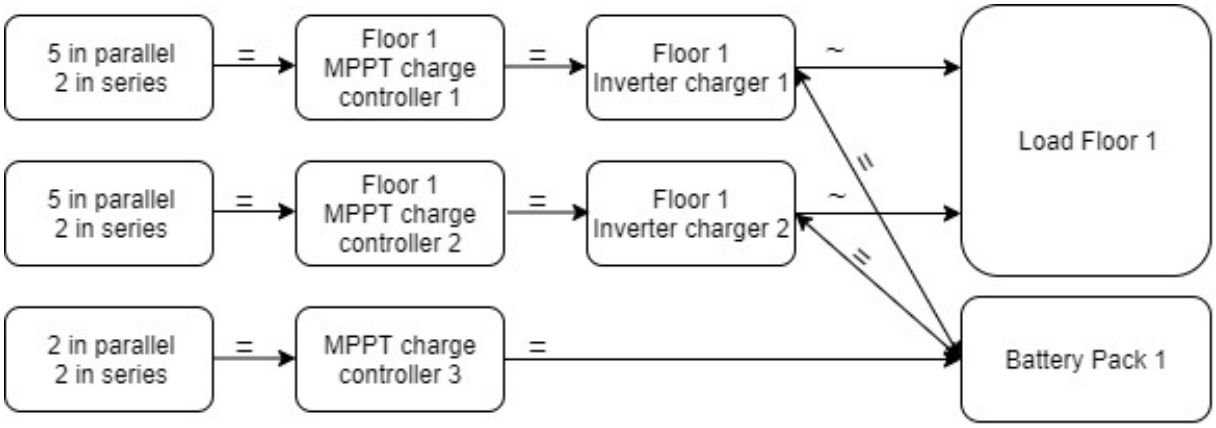

Figure 5.1: Representation of the assembly scheme of the PV system for floor 1

Describing the entire system, the PV panels are installed on the roof with a roof coverage of 34.8% in a total of 72 panels. In each floor there are 3 MPPT charge controllers, 2 inverter chargers and a battery pack with 3 batteries. Since the building has 3 floors, the final configuration of the system will have 72 panels, with 60 of them connected to 6 MPPT charge controllers connected to 6 inverter chargers and the remaining 12 connected to 3 MPPT charge controllers and 3 battery packs with a total of 9 batteries.

Choosing each specific model of inverter and MPPT, one had to consider the electrical properties of all the devices. Table 5.1 shows the specifications of a PV panel separately and the specifications of the entire PV system as a whole. Table 5.2 shows the specifications of the chosen model for the inverter charger and for the MPPT charge controller. From table 5.1, the PV system have a MPP voltage of 63.4 V, thus the inverter and the MPPT had to operate with an input voltage range compatible. From table 5.2, the inverter operates with a voltage range compatible to the system's MPP voltage and with a maximum

continuous power of 3500 W, thus, using equation 3.5, the maximum input current for the inverter is 55.2 A, comparing this value with the MPP output value of the PV panels, 47.35 A, one concluded that the device is compatible with the system. From table 5.2, the MPPT have a operating voltage range compatible with the system's MPP voltage, this voltage is between the minimum and maximum solar functional voltage recommended for the system, as long has battery voltage is lower than 63.4 V. The maximum power fed by the system to each MPPT connected to an inverter is 3000 W, and to each MPPT connected to a battery pack is 1200 W, thus, the PV system does not exceed the maximum power input (at STC) of both devices. The inverter and the MPPT are ready to be connected to a battery with a nominal voltage of 48 V.

PV Panel		PV System	
Brand	LG	Peak Power [kW]	21.6
Model	LG300S1C-A5	MPP Voltage [V]	63.4
Peak Power [W]	300	MPP Current (2x5 set) [A]	47.35
MPP Voltage [V]	31.7	MPP Current (2x2 set) [A]	18.94
MPP Current [A]	9.47	Open Circuit Voltage [V]	77.8
Open Circuit Voltage [V]	38.9	Short Circuit Current (2x5 set) [A]	50.35
Short Circuit Current [A]	10.07	Short Circuit Current (2x2 set) [A]	20.14
Efficiency	17.50 %	Price [€]	14 572.80
Price [€]	202.40		

Table 5.1: Specifications of the PV panels and PV system

Inverter		MPPT	
Brand	Studer	Brand	Studer
Model	XTM 4000-48	Model	VT-65
Continuous Power @ 25°C [W]	3500	At Nominal Battery Voltage [V]	48
Input Voltage Range [V_{DC}]	38 - 68	Maximum Solar Power Recommended (@ STC) [W]	4000
Maximum Input current for MPP Voltage [A]	55.2	Maximum Open Circuit Voltage [V]	150
Maximum Efficiency	96%	Maximum solar functional voltage [V]	145
Nominal battery voltage [V]	48	Minimum solar functional voltage [V]	Above battery voltage
Maximum charging current [A]	50	Operating voltage range [V]	7 - 68
Price [€]	2020	Efficiency	$>$99 %
		Price [€]	602

Table 5.2: Specifications of the inverter and MPPT

The peak power of the new PV system is 21.6 kWp, having 7.2 kWp per floor, the MPP operating voltage is 63.4 V, the MPP input current for the inverter is 47.35 A and the MPP input current for the MPPT is 18.94 A.

5.2 Re-sizing the power cables

In this new operational design of the PV system, it is necessary to re-size the power cables. These, will connect all the components of the system. Since there are new devices and the devices are distributed per floor, the power cables connecting the panels to each device must be reassessed. The assumption considered per floor, was that the two inverters, the three MPPTs and the battery pack, were placed together in the same location. This way, the cables that transport energy from a set of PV strings to the MPPTs of a certain floor have the same length, note that the length is different for every floor. With the previous assumption, it is possible to neglect the losses in the power cables that transport energy between the MPPTs and inverters, MPPTs and battery packs and between inverters and batteries, since the devices are placed together, the power cables are small, thus they have a very low thus, negligible, electric resistance. The cables that connect the PV strings to the inverters and that connect the inverters to the load are represented in figure 5.2, the DC side of the inverters, has one cable per MPPT and the AC side, has an output of three cables per inverter. Direct current flows in nine power cables and alternate current flows in eighteen power cables.

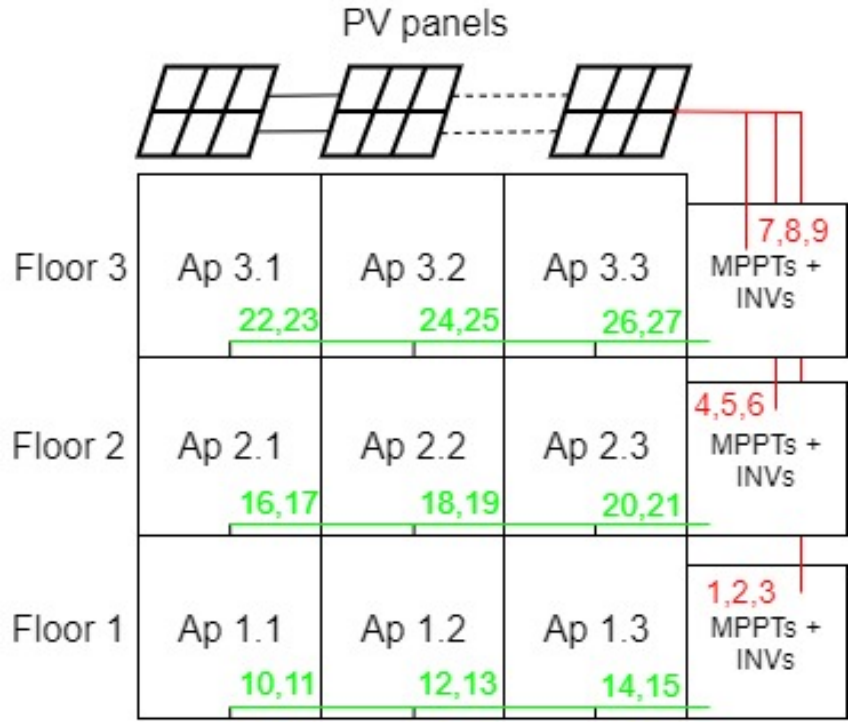

Figure 5.2: Scheme of the power cables connections in the building for the new system

Using figure 5.2 to identify the cables, the length estimated for each cable is given in table 5.3.

DC side		AC side	
Cable number	Estimated length [m]	Cable number	Estimated length [m]
1,2 and 3	102	10, 11, 16, 17, 22 and 23	25
4, 5 and 6	95	12, 13, 18, 19, 24 and 25	75
7, 8 and 9	88	14, 15, 20, 21, 26 and 27	125

Table 5.3: Length estimation for the power cables in the new system

The DC current that flows in the power cables, in this system flows from the PV strings to an MPPTs and then to an inverter, and it's now higher, thus the cross-section of the power cables on the DC side must be higher, the cross-section chosen for the power cables connected to the MPPTs which then will connect to an inverter, from appendix A.3, have a value of 16 mm^2, since the value for MPP current is 47.35 A and the value for short circuit current is 50.35 A. The maximum admissible current for this cable is 68 A. The cross-section chosen for the power cables connected to the MPPTs that will connect to a battery pack, from appendix A.3 have a value of 4 mm^2, since the value for MPP current is 18.94 A and the value for short circuit current is 20.14 A. The maximum admissible current for this cable is 28 A. Some security margin was assured while sizing the power cables.

Although the cross-section of the cables was chosen considering the operational limitations of the system, it must be ensured that these cross-sections are in compliance with the regulations for Cable Fire Safety. Support documents such as the Technical Guide [12] of the Portuguese agency, *Direção Geral de Energia e Geologia* , and the product specification document [13] (*Especificação de Produto, Nota CPR v1*) of Cabelte, S.A., are in compliance with the European regulations (*Regulamento (EU) nº 305/2011* and *Regulamento Delegado (EU) nº 364/2016*) and can be used to ensure that the power cables are, as well, in compliance with such regulations.

The specifications of this new design ensure that each floor has 2 inverters, thus, the inverters are not placed at the bottom of the building, this results in shorter power cables on the AC side, thus, lower cable electric resistance. To estimate the section of the power cables in the AC side, it's necessary to compute the RMS value of the current. This value for the current on the AC side is obtained in section 5.3.

5.3 Assessment of the power losses in the new system

Since the design of the system was changed, the power losses must be re-assessed. Note that, as in section 3.5, the PV power used to assess the power losses is the hourly average of energy generated during production hours of the coldest day ($P_{pv} = 7344.5$ W), as observed in figure 5.3. The methodology used for this computations is the same as in section 3.5. However, a slight change must be considered. In this system, the energy will be stored, thus on the AC side, the power transported will be limited by the load needs. In this case, P_{load} is equal to the energy needs of the building ($P_{load} = 3375.3$ W), I_{rms} must be computed using equation 5.1. The value used for P_{load} is the maximum load value for the coldest day.

$$I_{rms} = \frac{P_{load}}{3 \cdot U_{phase} \cdot cos\varphi} \tag{5.1}$$

The new results for power for the coldest day can now be computed. The RMS value of the current, I_{rms}, in each AC cable is equal to 1.02 A thus, the section of these cables is equal to $1.5mm^2$ with a maximum admissible current of 15.5 A. The total Joule power losses in the cables have a value of $P_{J_{cables}} = 136$ W, which can be related to the generation as a percentage loss: $P_{\%losses} = 2\%$.

The energy that is lost in the power cables is lower than 10%, the losses transporting energy in the

power cables do not have significance for the formulation of the problem, thus, they were neglected.

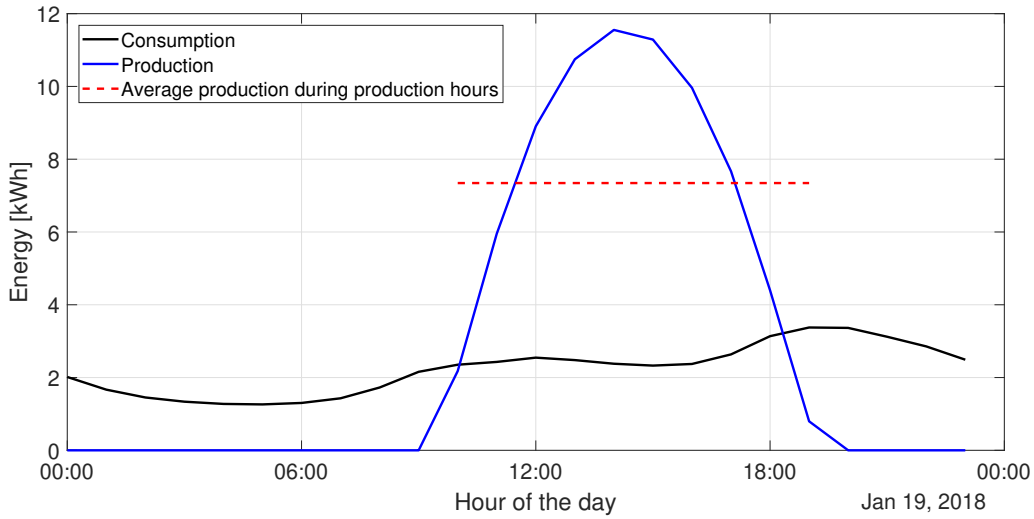

Figure 5.3: Hourly energy consumption, production and average production during production hours for the coldest day of the year considering the new consumption profile and the new system

5.4 System's performance without energy storage

In a first approach the viability of the system was tested without storage devices. One must note that the peak of production, in a PV system, is during lunch time, however, as stated in section 4, the peaks of consumption are around 8 a.m. and around 9 p.m. Since there are no batteries and the PV system is the only source of energy, one can expect that the PV system will not be enough to satisfy the demand of energy. This raw test of the system is mainly used to compute the total surplus of energy produced after the demand is met and the total deficit of energy when the demand is not met. At this stage, the load of each apartment is considered equal to the hourly average one, thus, each floor has the same characteristics for energy consumption.

In order to test the system described in section 5.1 some assumptions were considered. The power train described for all floors was simplified to a general production PV plant with 21.6 kWp and the same panel properties. This PV plant is connected to a general inverter with 96% efficiency, delivering electricity to all of the 3 floors. The energy that reaches the load was compared with the energy needs of the building. The surplus and deficit of energy were computed. The time spam for computations was 2 years and 3 months starting in January 1^{st}, 2018. However, for this analysis it was reduced to one year, starting in the second Winter (December 21^{st}, 2018). This restriction was chosen in order to analyze the PV system in a near-stationary condition. In the beginning of the computations the battery starts fully charged, but this does not happen in practice, the battery of the system may not begin fully charged in the first day of a certain year thus, the near-stationary behavior of the system would not be comparable to the behavior in the first year. In figure 5.4 one can observe the amount of energy at the load after the building's needs are met. To compute the total surplus of energy being supplied to the building when the

needs are satisfied, one can sum all the positive points and to compute the deficit, all the negative ones. The total surplus of energy was 28205 kWh and the total deficit of energy was 7216.9 kWh.

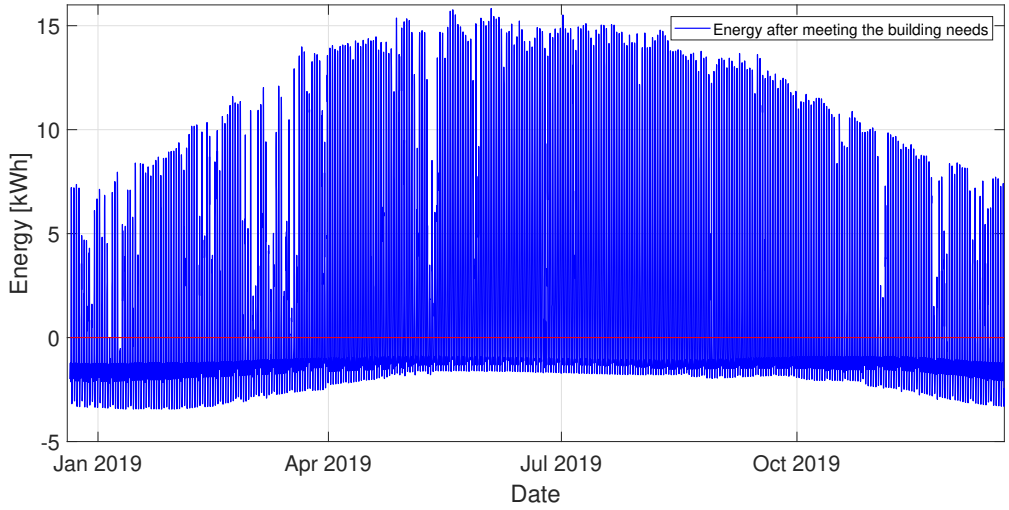

Figure 5.4: Surplus and deficit of energy for the second year

This is a representative value that show that the production is enough to cover all the building needs, however, that is not possible because the energy is not being stored. The coldest day in the 2 years and 3 month spam of the analysis was January 19^{th}, 2018 the analysis for this day aims to show that the produced energy was enough to satisfy the consumption. Figure 5.5 shows the difference between peak of production and peak of consumption during the coldest day of the year. If the energy produced in a day with this profile was stored, it would be enough to satisfy the consumption and the load at the building would be leveled. The total production for the coldest day was 73.4 kWh and the total consumption for the same day was 53.5 kWh. Since the energy is not being stored, the energy needs of the building are only met when the production is higher than the consumption and there is a surplus of energy at the load not being used.

5.5 Integrating batteries as energy storage devices

The use of batteries to store energy is a solution that aims to ensure that the building has energy being delivered 24 hours a day. Several aspects must be considered when choosing and sizing a battery, such as the type of metal used in the battery's cells, the chemical composition of the cells, the required capacity, the power that it can deliver, the max input current the compatibility with the other devices. The battery used was a lithium ion battery, because lithium has a high energy density, the composition is lithium nickel cobalt aluminum oxide ($LiNiCoAlO_2$), because it is one of the compositions with lithium with a high energy density. Each floor of the building have a pack of 3 batteries, with a total of 30.18 kWh capacity per floor. The system was designed with this capacity to ensure that if the PV system was off during the coldest day, each battery pack would be able to sustain the needs of each floor for the entire day, if they were charged to at least 80%.

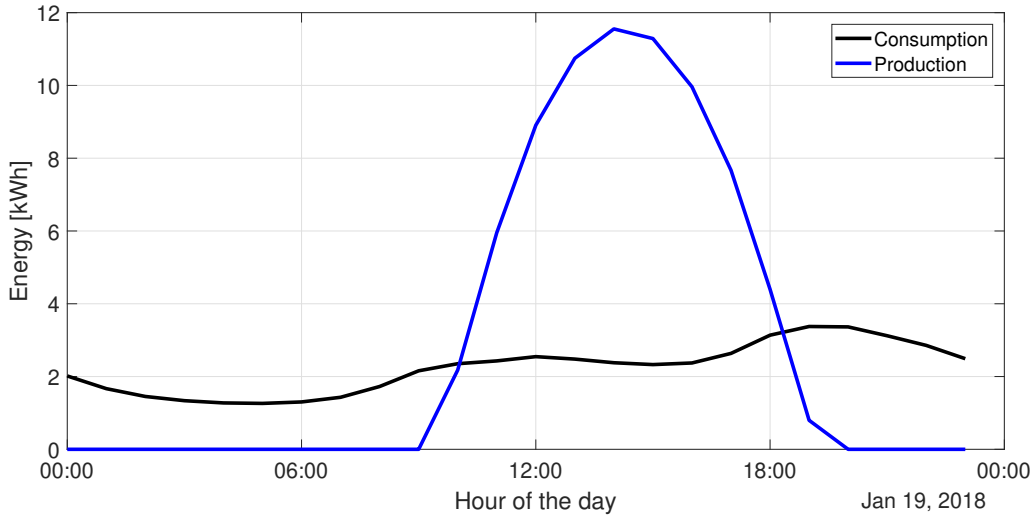

Figure 5.5: Hourly energy consumption and production for the coldest day of the year

Battery	
Brand	BMZ
Model	ESS X
Energy (nom,/usable) [kWh]	10.06 kWh / 8.05 kWh
Nominal voltage [V]	54
Charge end voltage [V]	61.5
Discharge end voltage [V]	45.0
Max. charge current [A]	90
Max. discharge current [A]	300 (3 sec)
Max. discharge power [kW]	18
Weight [Kg]	99
Battery Chemistry	Li-Ion NCA
Discharge depth	80 % DOD
Full cycles	5000
Energy Density [Wh/Kg]	101.6
Price [€]	4588.00

Table 5.4: Specifications of the battery

Each battery has a maximum power output of 18 kW. The MPP operating current of the system is 47.35 A, the maximum input current of each battery is 90 A, the maximum charging current of the inverter charger is 50 A and the maximum output current of the MPPT charge controller is 65 A, all the devices are compatible. The operational range of the battery goes from 45 V to 61.5 V, the voltage required by the inverter and MPPT was 48 V thus, the battery satisfies those requirements. The DOD is imposed by the manufacturer as 80% DOD, the variation of charge will be assumed from 100% to 20%. The battery has a cycle life of 5000 full cycles.

When batteries were implemented, the energy fluxes in the build had to be assessed and prioritized. The energy produced by the PV system had the priority to feed the building. The energy needs of the building were assessed when the produced energy was allocated. If the energy produced was bigger than the building's needs, the surplus of energy would flow into the battery, however, if it was less than the building's needs, the difference would flow from the battery into the building. The battery's capacity was assessed as well. When feeding the battery with surplus energy, if the battery reached full capacity, the system was limited or even cut-off since there would be no way of storing the energy and the extra energy would only be accounted for. The same assessment was made if the battery reached it's lower limiting capacity when feeding the building, the system would be shut off and the battery would remain at it's lower limiting capacity, in this case, the floor where the battery was placed would not have it's energy demand satisfied.

The system now has the PV panels, the inverter chargers, the MPPT charge controllers and the batteries. It was tested for the same weather and load conditions as in section 5.4.

The surplus and deficit of energy in the building were analyzed again for the same time spam as in section 5.4, one year starting in the second winter and for the system with batteries, this allowed to check if the energy needs of the building were now satisfied. At this stage, the load of each apartment, as in section 5.4, is considered equal to the average one, thus, each floor has the same characteristics for consumption and battery's SOC along the analysis. Figure 5.6 shows that the energy needs of the residential building are almost entirely satisfied. However, there are certain critical periods of the year where the system is not enough to satisfy those needs. This occurs during Winter time and at the end of the fall season. In these periods it was expected that production would be lower due to the occurrence of clouds in the sky, thus low irradiance and that the load would be higher due to heating needs, resulting in a deficit of energy in the building.

In figure 5.7, there is a match between the days when the building had a deficit of energy and the days when the battery's level was at 20%. Since the DOD of the battery was 80%, the battery could not be discharged under 20 % and this resulted in a lack of energy being delivered to the building.

From figure 5.6 one could also observe that during summer time, there was a great surplus of energy, and matching with information from figure 5.7, it was when the battery's SOC was never below 80%. The purpose of this study does not analyze what happens to the surplus of energy.

A seasonal analysis was performed to assess the different behavior and response of the system under different weather conditions. Remember that this analysis starts in the second winter of the data computed, this allows to evaluate the system in a near-steady state condition.

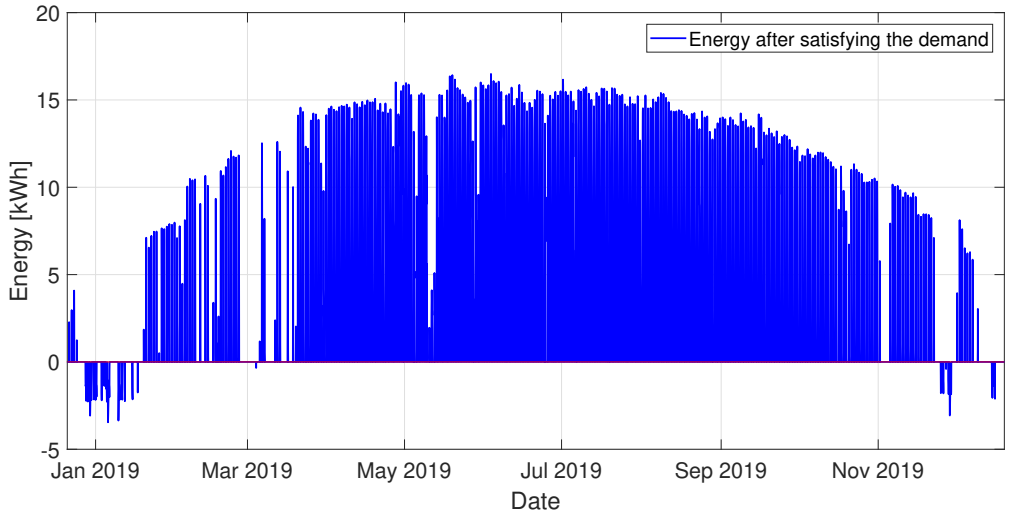

Figure 5.6: Surplus and deficit of energy along the 15 months in the building with batteries

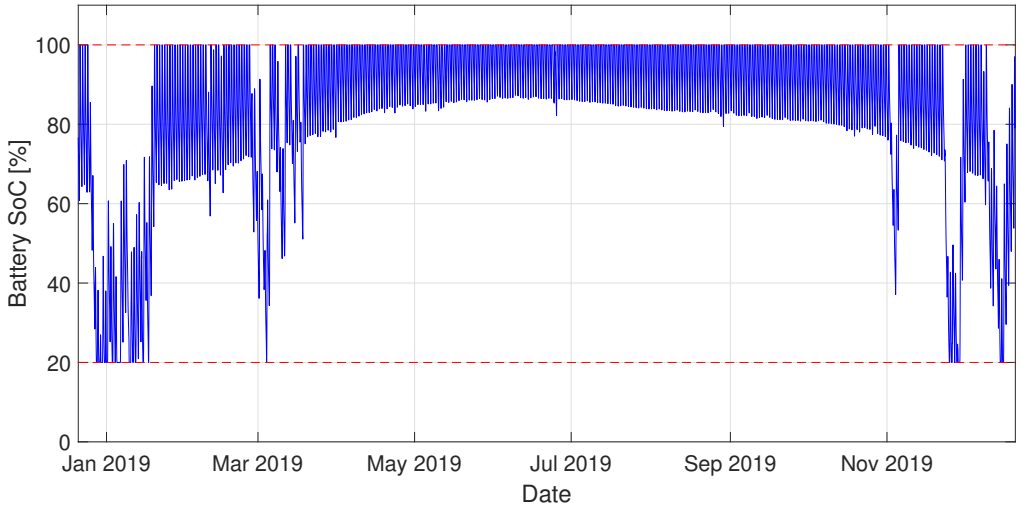

Figure 5.7: Hourly battery level for each floor along the year

5.5.1 Seasonal analysis

The production of energy in a PV system depends on weather factors, the three most important are irradiance, temperature and cloud cover of the sky. The irradiance that reaches a panel is influenced by the cloud cover, and the panel efficiency depends on the cell's temperature and this depend on irradiance and ambient temperature, as explained before in equation 2.3.

The first season in analysis is the Winter season, figure 5.8, shows the relation between cloud cover, useful irradiance (which is the irradiance that is felt by a solar panel) and production. It is possible to note that when the cloud cover is at 100% or near, the useful irradiance decreases and the production decreases with it. For instance, in the end of February, the cloud cover is at 0% and the useful irradiance is very high, so is the production. However, in the beginning of March, when it is observer a sky cloud cover of 100%, the useful irradiance decreases and does the production.

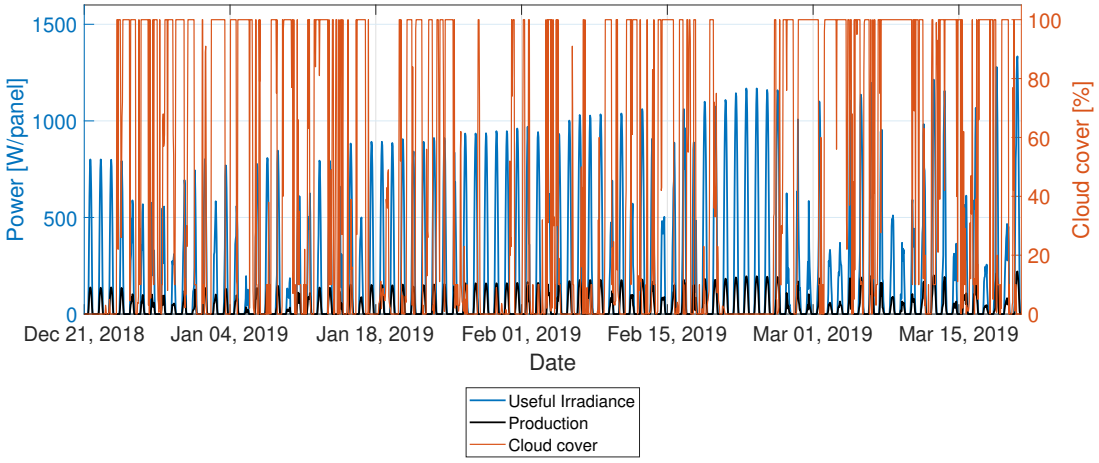

Figure 5.8: Hourly irradiance, production and cloud cover for the Winter of 2019

Figure 5.8 also describes a slight increase trend of the irradiance thus, the production.

The efficiency of the PV cells is always changing with the weather conditions as well, since it depends on the ambient temperature, it is possible to note that in the end of February it reaches it's minimum and maximum for this season, this happens when the temperature reaches it's maximum and minimum, respectively, for this season.

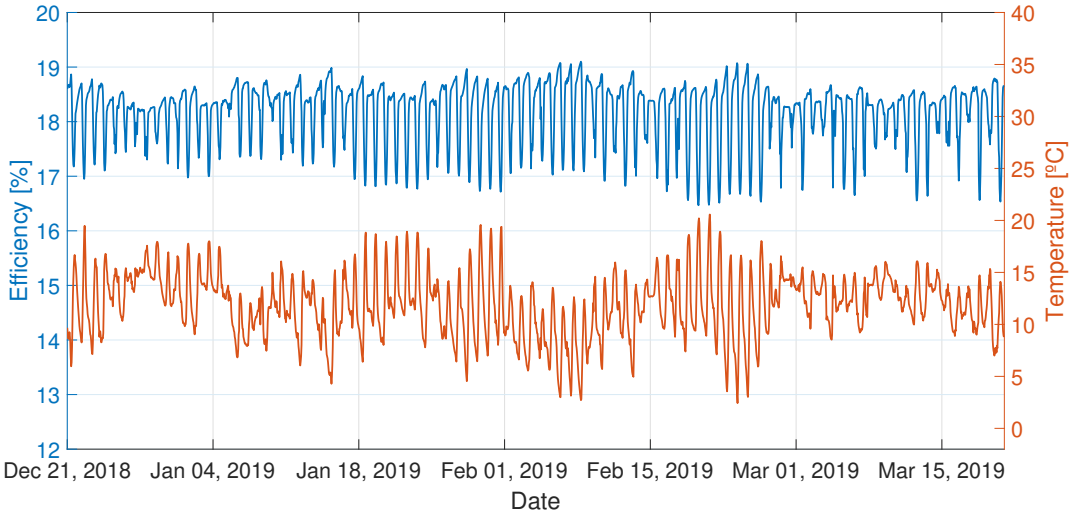

Figure 5.9: Hourly, cell's efficiency and ambient temperature for the Winter of 2019

Analysing the entire production of the PV system it is possible to note that it is much higher than the consumption, however, if there are a few cloudy days the production decreases drastically. Figure 5.10 describes the profile for production of the entire PV system and for the consumption of the whole building. The consumption shows a slight trend to decrease at the end of the Winter.

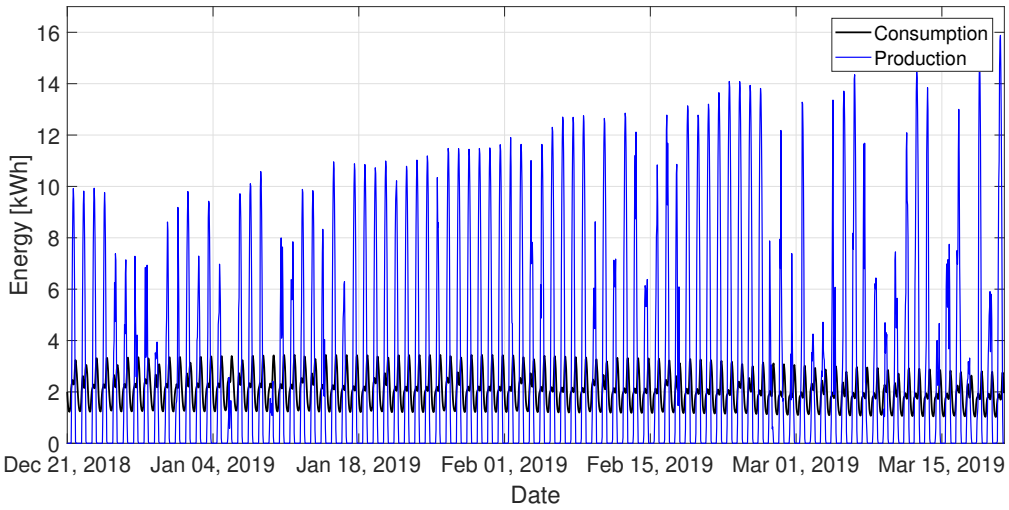

Figure 5.10: Hourly production and consumption for the Winter of 2019

The battery's SOC will suffer change depending on the needs of the building. The battery's capacity is limited to never decrease below 20%. Figure 5.11 shows that the SOC of the battery reaches 20% in the end of December, beginning of January and again in the beginning of March, when this happens, the system has a deficit of energy, and the building's needs are not met. For this season the battery cycle count increases around 35 cycles.

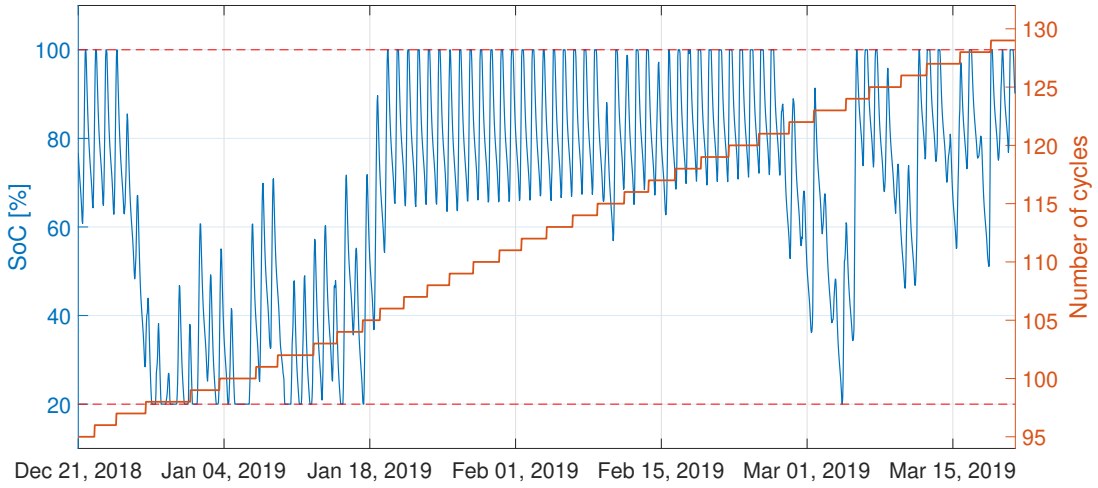

Figure 5.11: Hourly battery's SOC and cycle count for Winter 2019

Linking information from figures 5.8, 5.10 and 5.11, it is possible to observe that cloudy days have a consequence resulting in low production of the entire PV system, since this happens, the system has to use the battery as an energy source, thus the battery's SOC decreases abruptly. In the end of December of 2018, beginning of January of 2019 and in March of 2019, such occurrence was observed.

During the Spring of 2019, there is lower occurrence of clouds. Figure 5.12 shows that cloud cover is at a 100% for less time and that the useful irradiance per panel has low variation from day to day. The production shows, as well, a behavior with low variation. It is still possible to observe that high cloud cover results in low useful irradiance and low production for example around mid May.

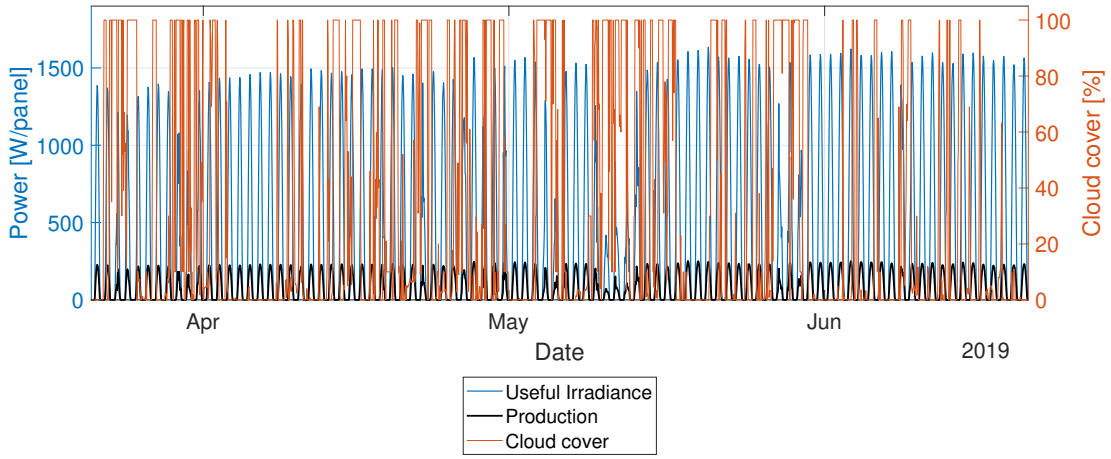

Figure 5.12: Hourly irradiance, production and cloud cover for the Spring of 2019

In this season the ambient temperature describes a trend to increase, thus, as shown in figure 5.13, the efficiency show an opposite trend, meaning, a trend to decrease. Comparing the beginning and the end of the season, the temperature shows a difference of around 30 °C and the efficiency of around 2%.

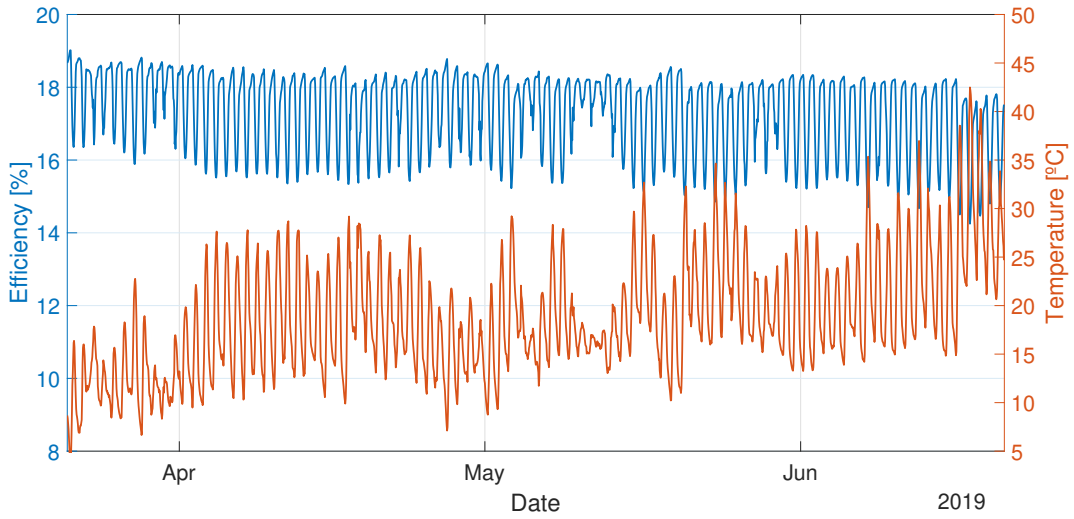

Figure 5.13: Cell's efficiency and ambient temperature for the Spring of 2019

Figure 5.14 shows that the production of the entire system tends to remain with low variation, and that it is higher when compared to the Winter season.

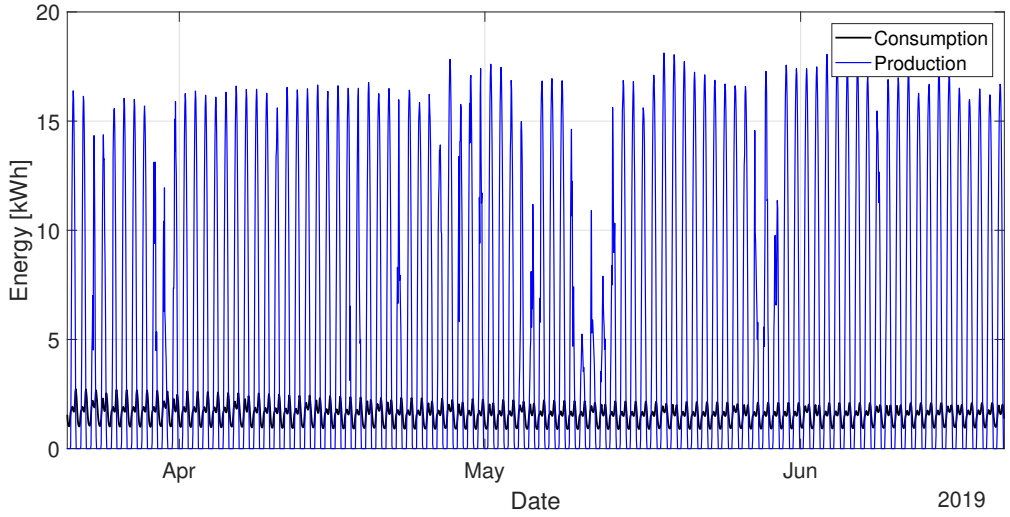

Figure 5.14: Production and Consumption for the Spring of 2019

The battery's SOC is almost always higher than 80% and shows a cyclic daily behavior, as shown in figure 5.15. The battery cycle count increases around 20 units for this season.

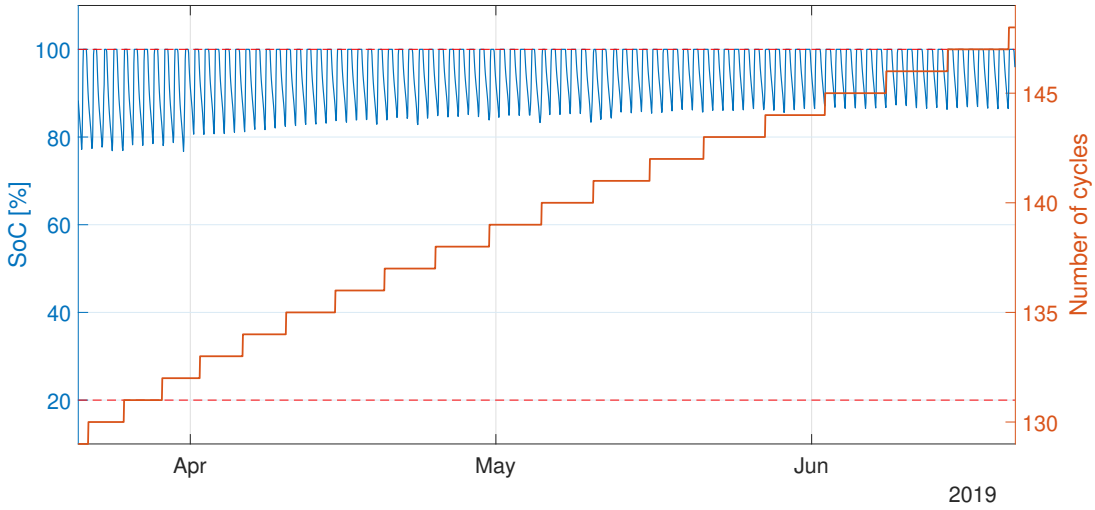

Figure 5.15: Battery's SOC and cycle count for Spring 2019

Connecting information from figures 5.12 and 5.14, it is possible to observe, again, that the total production of the system is lower when there is an intense occurrence of clouds in the sky.

From Spring to Summer it is again possible to observe, from figure 5.16 a decrease in the occurrence of clouds, thus the irradiance is high and has a stable behavior, as well as the production. In figure 5.16, the irradiance shows a trend, in the end of the season, to decrease.

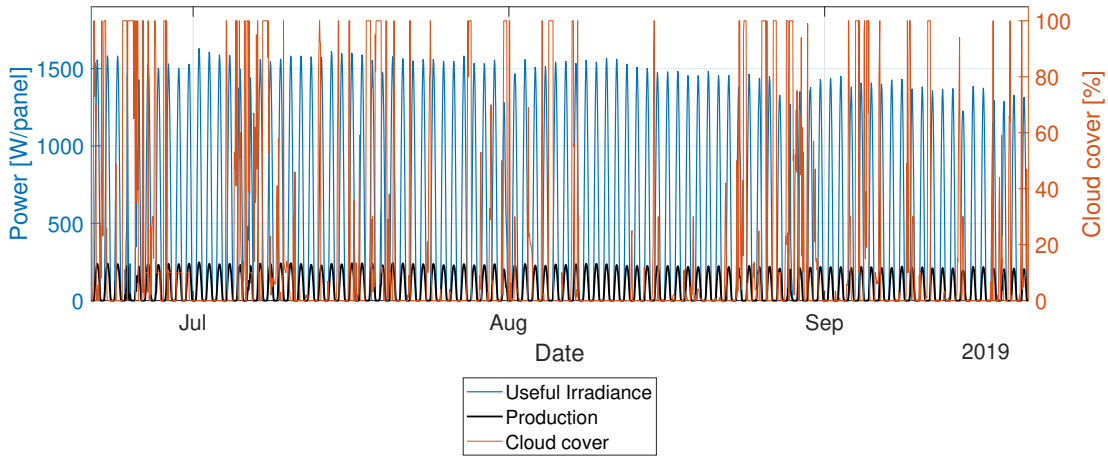

Figure 5.16: Irradiance, production and cloud cover for the Summer of 2019

The temperature and efficiency describe a stable profile during this season, as it can be observed in figure 5.17.

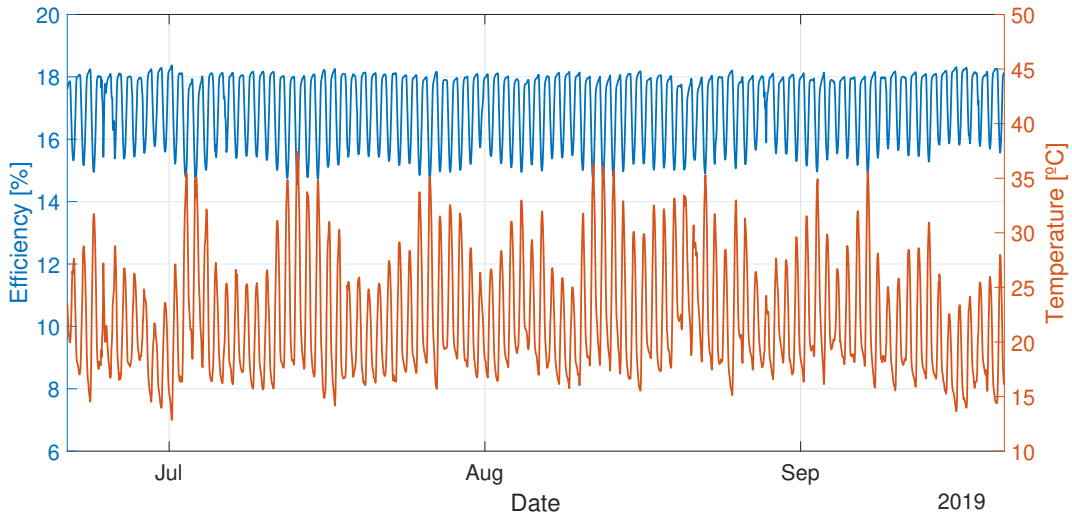

Figure 5.17: Cell's efficiency and ambient temperature for the Summer of 2019

From figure 5.18, it can be observed that the total production of the system is very high during this season, however in the end of the season it shows a trend to decrease. Moreover, for this season the consumption, describes a constant behavior.

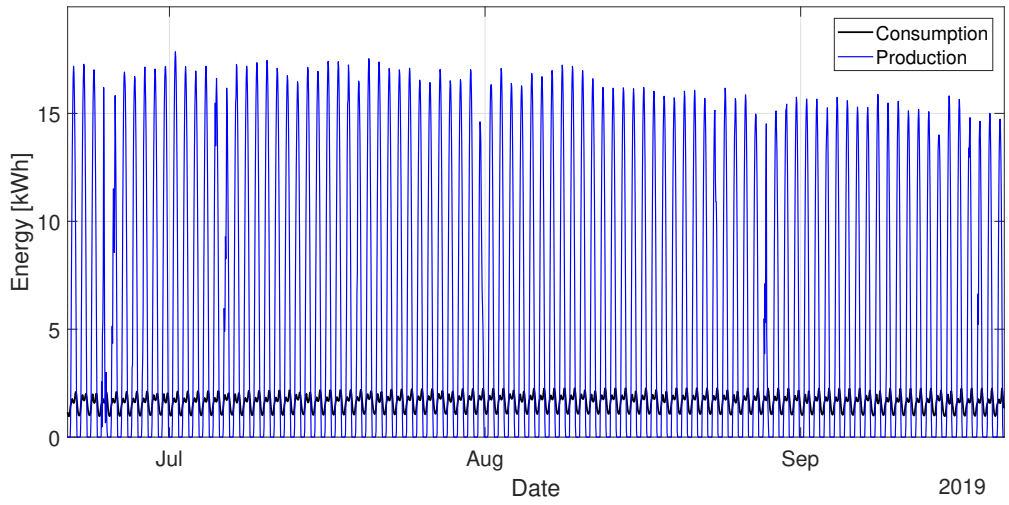

Figure 5.18: Production and Consumption for the Summer of 2019

For the Summer season, alike Spring season, the battery's SOC is almost always higher than 80%, as it is observed in figure 5.19. The cycle count for this season increases around 20 units.

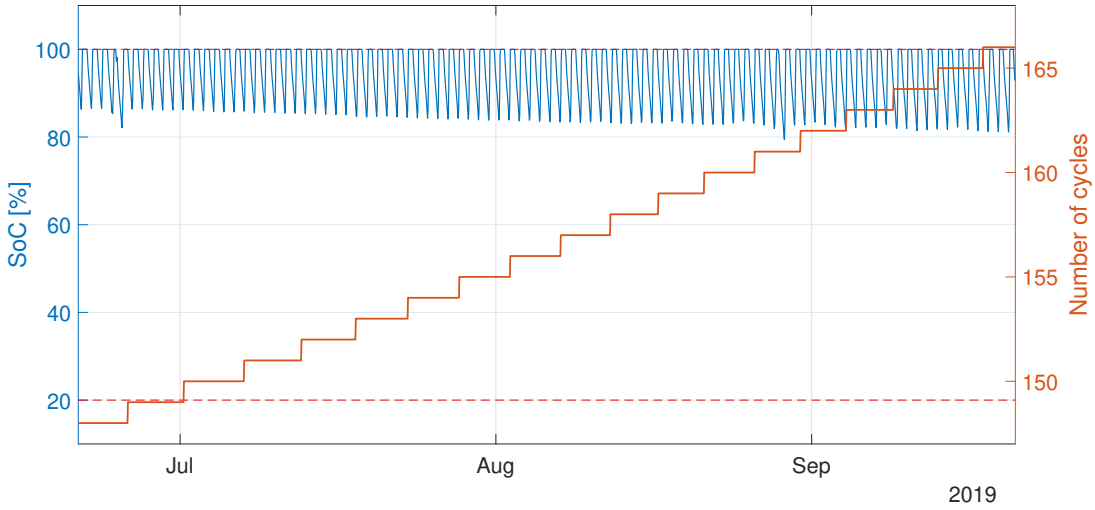

Figure 5.19: Battery's SOC and cycle count for Summer 2019

The Fall season compared to the Summer season has more occurrence of clouds in the sky. From figure 5.20, the production per panel show a trend to decrease along the entire season, and in cloudy days, the irrandiance and the production decrease significantly.

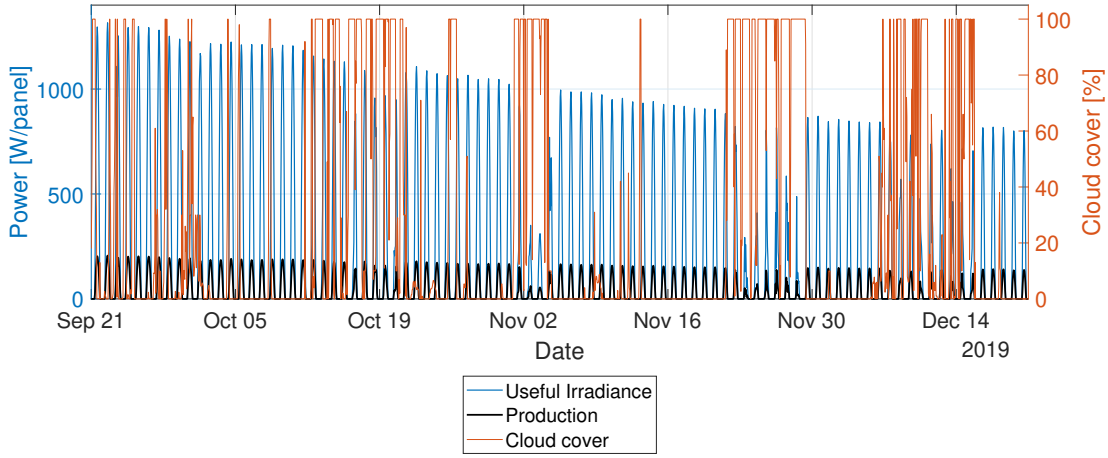

Figure 5.20: Irradiance, production and cloud cover for the Fall of 2019

In figure 5.21, a trend of ambient temperature decrease can be observed. This results in an increase of cell's efficiency. Comparing the beginning and the end of the season, one can state that the difference in efficiency is around 1% and the difference in temperature is around 15 ^{o}C.

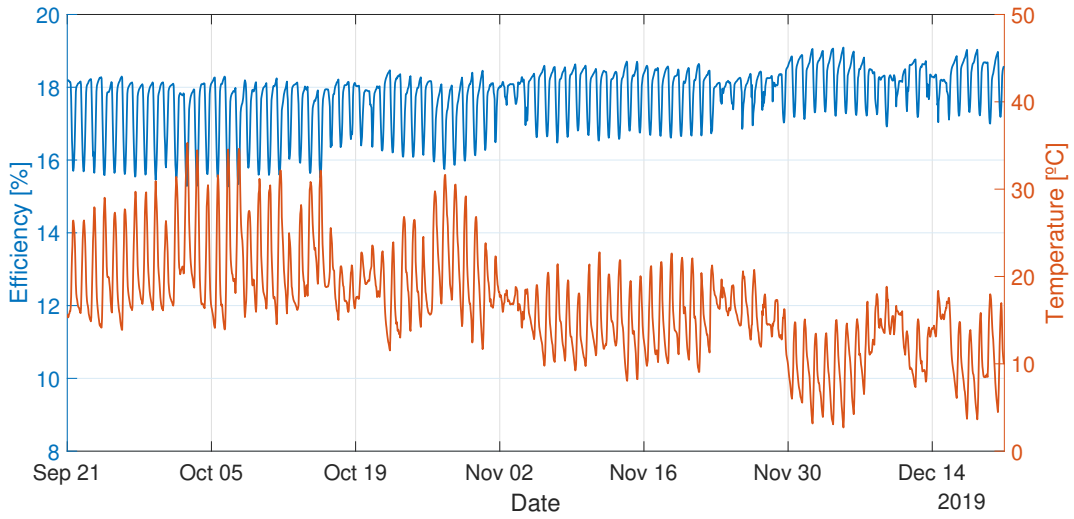

Figure 5.21: Cell's efficiency and ambient temperature for the Fall of 2019

The total production of the system shows a trend to decrease along the entire season, as observed in figure 5.22 and the production a trend to increase.

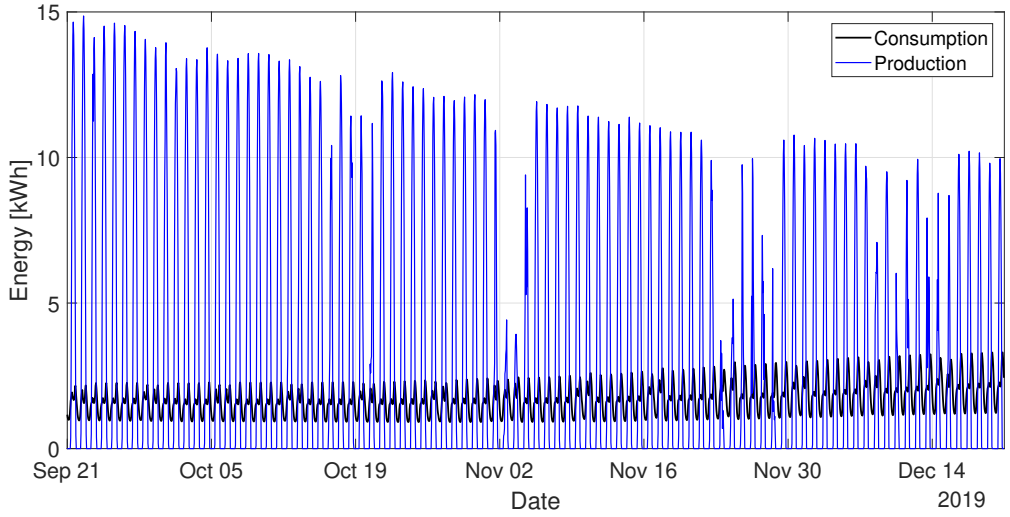

Figure 5.22: Production and Consumption for the Fall of 2019

From figure 5.23 it is possible to observe that the battery's SOC variation increases and that there are days where the battery has to feed a lot of energy to the building. The cycle count for this season increases around 30 units. The last value for the cycle count in this analysis is 195 cycles.

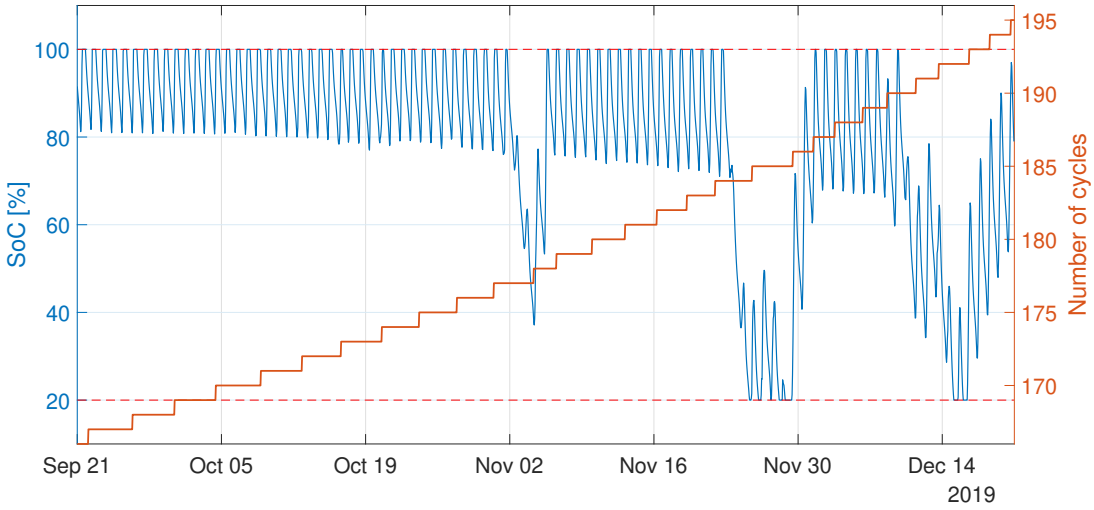

Figure 5.23: Battery's SOC and cycle count for Fall 2019

Connecting information from figures 5.20, 5.21, 5.22 and 5.23, it is possible to observe that the decrease in temperature had a consequence on higher consumption to satisfy heating needs, it is also possible to observe that in the beginning of November, end of November and mid December, there were intense occurrences of clouds in the sky thus, the total production of the system decreased. During this periods, the battery had to be used as a main source of energy to the building. This resulted in an abrupt decrease of the battery's SOC, sometimes even reaching the lower limiting capacity of 20%. Note that when the battery reached this capacity, the system had a deficit of energy and the energy demand of the building was not satisfied.

The season where it was noted a higher battery's cycle count was the Winter season. The Winter season and the Fall season, are the seasons where the system experienced a deficit of energy, in this seasons, the battery reached, at least one time, it's lower limiting capacity of 20%.

The assembled system was not yet fully reliable to operate on its own has it was very sensible to irradiance variations during the Winter and Fall seasons. In order to complement the system, some emergency measure must be implemented to allow for this PV system to properly function without jeopardizing the energy consumption of the building's residents. At this stage, the system was not enough to ensure that all the energy needs were fully satisfied.

With a consideration of continuity of the system's conditions and characteristics between years and seasons, the model developed can analyze and predict the behavior of the entire system throughout the years.

5.5.2 Critical day's analysis

The energy analysis of the battery was performed for critical days of the year. In this analysis the hourly production and consumption were assessed, as well as the battery SOC. The coldest day of the year was assessed because is a day where the load is expected to be higher to ensure thermal comfort in each apartment with heating devices. The hottest day of the year was assessed because

is a day where the load is expected to be higher to ensure thermal comfort in each apartment with cooling devices. The cloudiest day of Summer and Winter, were assessed because the production was expected to decrease during these days due to a lack of irradiance.

For the coldest day of the year, from figure 5.24, the battery's SOC decreases until production is higher than consumption, at this stage, it increases to reach 100% around 3 p.m. At the end of the day, after 6 p.m., the battery's SOC will start to decrease again as the production is smaller then the consumption. It is possible to say that for this day, the system has excess of energy while the SOC is at 100% and the production is bigger than the consumption.

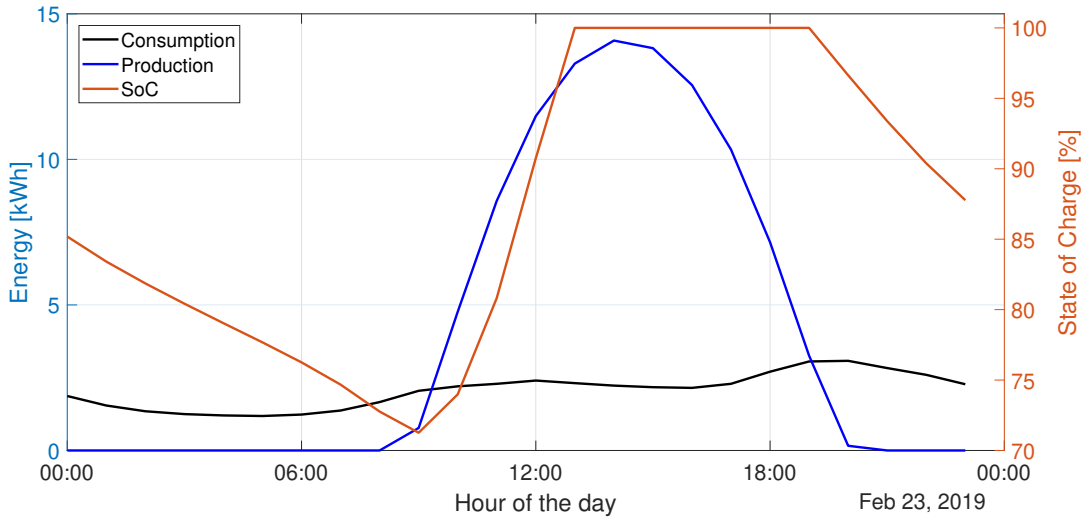

Figure 5.24: Hourly energy production, consumption and battery's SOC for the coldest day of the year

For the hottest day of the year, from figure 5.25, it is observed that the production is much higher than consumption during sunshine hours. In the begging of the day the battery's SOC decreases, but since production is very high, it rapidly reaches 100% during the morning and it remains at 100% during sunshine hours.

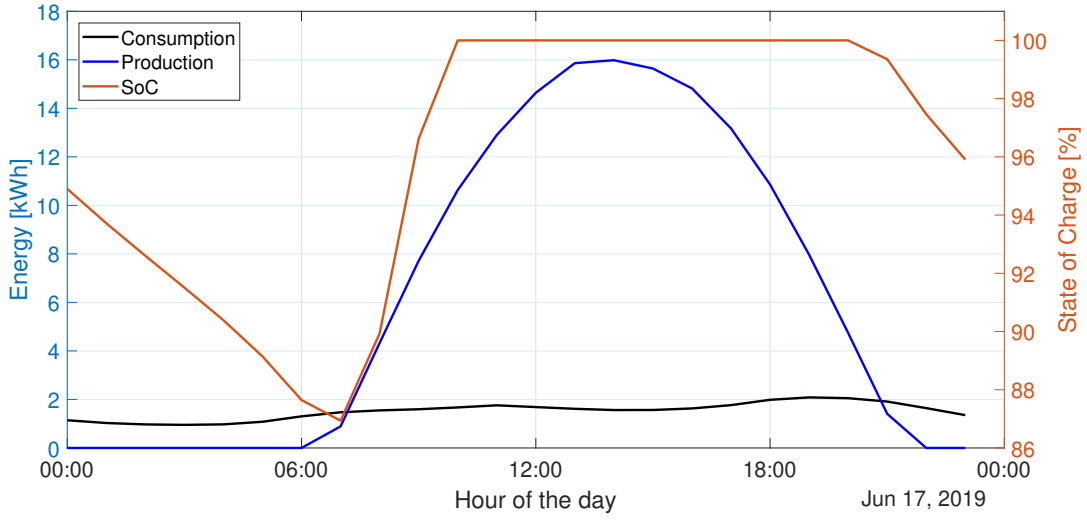

Figure 5.25: Hourly energy production, consumption and battery's SOC for the hottest day of the year

This shows that there is an excess of energy being generated that is not being used to feed the load or the battery.

For the cloudiest day of the Winter, from figure 5.26, the production is smaller than the consumption for the entire day. The battery's SOC decreases during the entire day, even during production hours where the decrease is reduced. Around 10 p.m. the battery's SOC reached 20%, the lower limit, thus, there is a lack of energy in the system and the building's consumption was not satisfied.

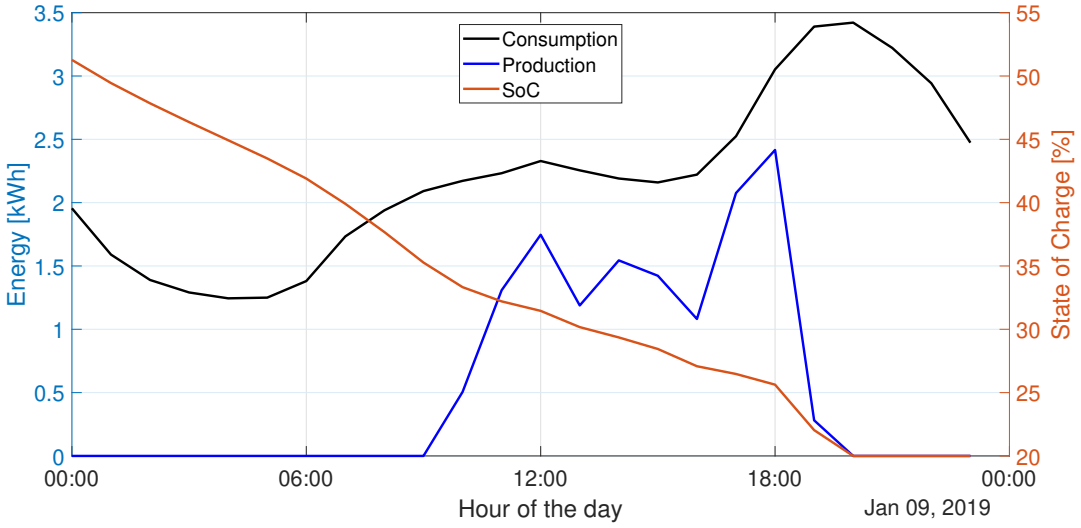

Figure 5.26: Hourly energy production, consumption and battery's SOC for the cloudiest day of Winter

For the cloudiest day of Summer, from figure 5.27, the production shows an unstable behavior, however, it is almost always bigger that consumption during sunshine hours, the battery's SOC increases during sunshine hours and reaches 100% at noon. This shows that there is an excess of energy being generated that is not being used nor stored.

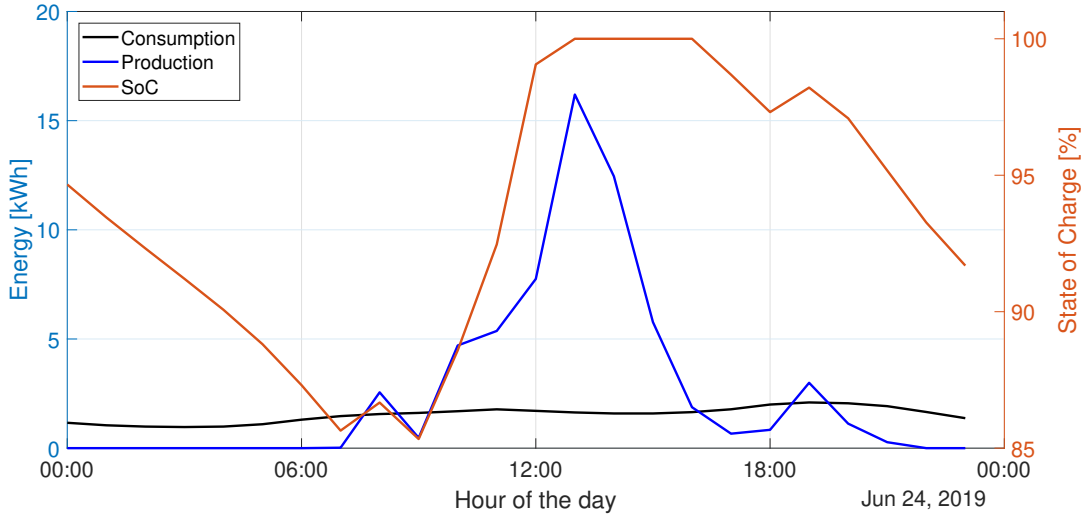

Figure 5.27: Hourly energy production, consumption and battery's SOC for the cloudiest day of Summer

Chapter 6

Micro combined heat and power plant

During the entire year that was analyzed in chapter 5, the energy system of the building with the PV system as the only source of energy and with batteries used for energy storage, was not enough to satisfy the total energy consumption of the building. In such analysis, the system could not supply the building for 185 hours and the total deficit of energy was 284 kWh, which represent around 2% of the hours and consumption of the year. In order to have a full steady supply of energy a new source of energy was installed in the building, a micro *Combined Heat and Power Plant* (CHP) that works on the principle of cogeneration. The fuel for this unit is natural gas and is supplied from the Portuguese natural gas grid. This device will only be used in case of emergency, operating as a generator of electric energy. Therefore, the device will be turned on only when there is a deficit of electric energy in the building. In practical terms this means that when the battery reaches its lower limit of 20 % SOC and the PV production is not enough to satisfy the energy needs in the building, the micro CHP will be immediately turned on. The heat generated by this micro power plant will not be assessed in this thesis, however considering its properties could increase the efficiency of the system and decrease the electricity demand from boilers and heating systems.

To chose the power of the micro CHP, the maximum load for the entire building was assessed, the generator must have a power higher than this value. The maximum load for all the nine apartments was 3.441 kW, thus, the generator must have a higher power capacity, the model chosen for the generator was XRGI 6 from EC Power with an electrical output power of 6 kW.

6.1 Assembly of the device in the system

Since this device will only be used in case of emergency, the priority for the energy generated is to satisfy the apartments needs, and any surplus of energy produced during the operation of the micro CHP will be fed into the batteries evenly. The physical links between the PV system and the micro CHP are the batteries and the load. When the generator is turned on, the system must consider all the energy generated and all the surplus of energy in order to compute the batteries' level. The connection scheme for the generator is described in figure 6.1. A controller will be responsible to ensure that the flow of

electric energy respects the priorities established above.

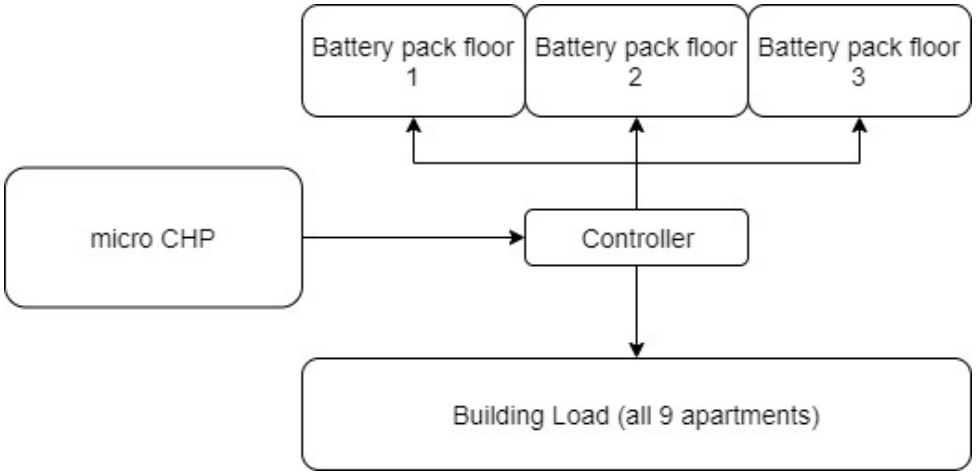

Figure 6.1: Representation of the electric connections for the micro CHP

6.2 Energetic analysis

Using the generator only in emergency conditions, in order to achieve zero deficit of energy, the generator worked for 49 hours, during the period in analysis, and produced a total amount of energy equal to 294 kWh. The number of hours required to operate the generator in order to achieve zero deficit is much lower than the number of hours where there was an occurrence of deficit, this happens because the excess energy that the CHP unit generates is stored in the batteries.

The system's performance using the PV system as the main source and the micro CHP as an emergency source was analyzed. The seasons where the system had deficit of energy were the Winter season and Fall season, those, will be discussed in section 6.2.1 and the critical days of the year will be discussed in section 6.2.2

6.2.1 Fall and Winter of 2019

During winter season, the generator was important to ensure that the building's energy needs were met. Figure 6.2, shows the total energy produced by the energy system in a hourly base, as well has the consumption and the energy produced by the generator. There were critical periods were the generator was very much needed to ensure a steady supply. The consumption was higher than production in several hours throughout the season and the emergency supply was used, since there was not enough energy stored to ensure such supply.

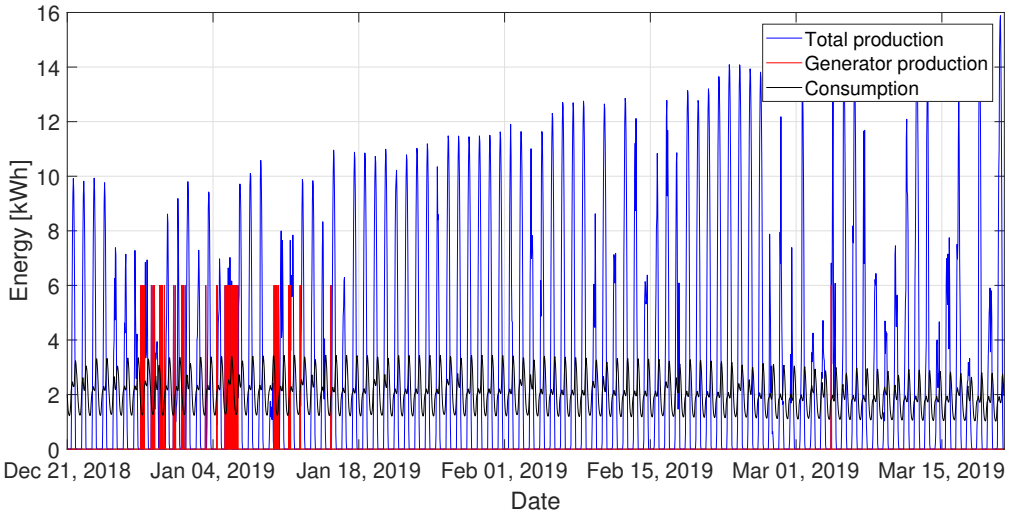

Figure 6.2: Hourly production and consumption for the Winter of 2019 with the micro CHP

During the hours that the generator was producing energy, it is possible to observe small oscillations in the battery's SOC. This can be observed in figure 6.3 and in more detail in figure 6.4, around January 5^{th} this happens because with the generator working at full capacity, supplying an output of 6 kWh per hour, after the building's energy needs were met, the surplus that was produced in that hour was used to feed the batteries.

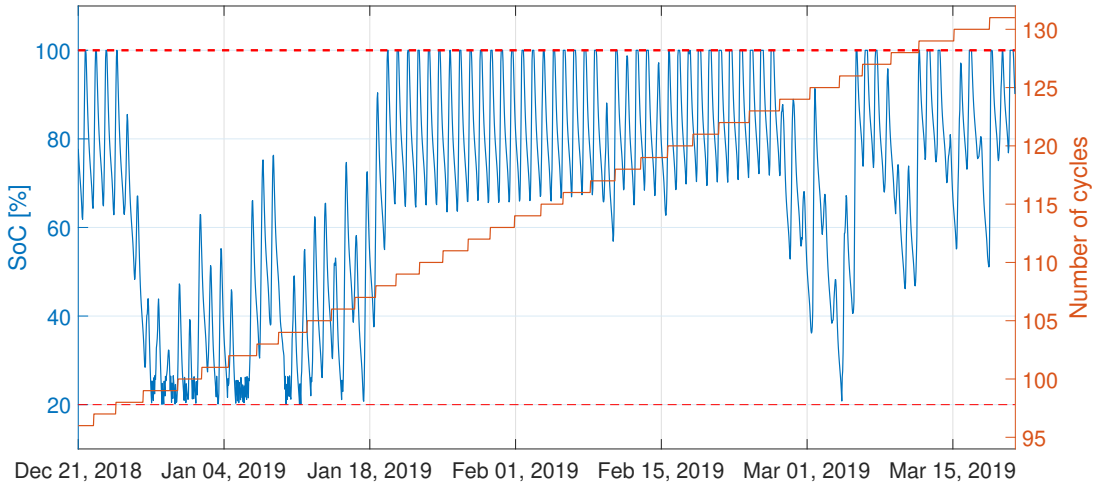

Figure 6.3: Hourly battery's SOC and cycle count for Winter 2019 with the micro CHP

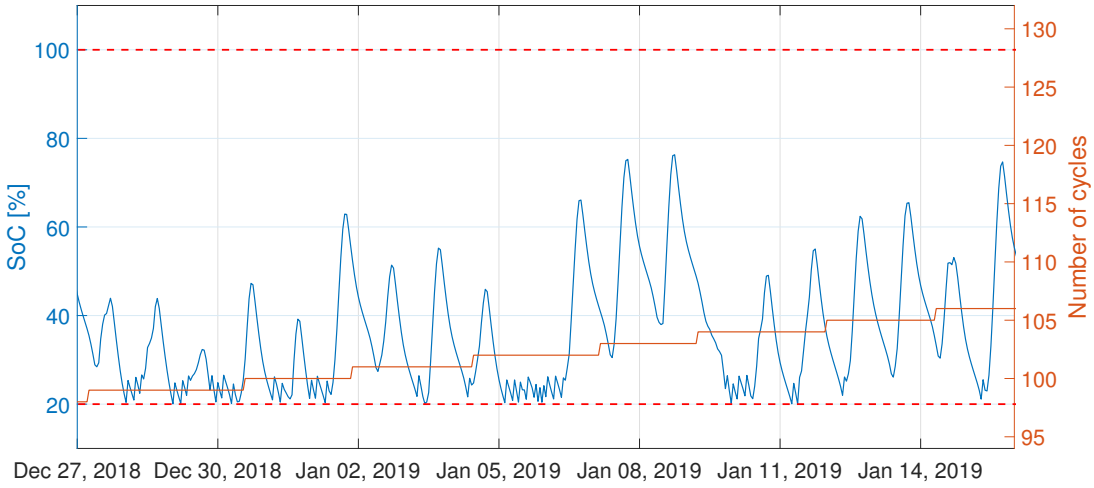

Figure 6.4: Hourly battery's SOC and cycle count for a period in the Winter of 2019 with the micro CHP

For the Fall season, as well as for Winter, the generator had an important role to ensure a steady supply where there was no deficit of energy. Described in figure 6.5, this happened in the end of November and mid December for several hours, due to the production being lower than the consumption and because there was not enough energy stored to ensure supply.

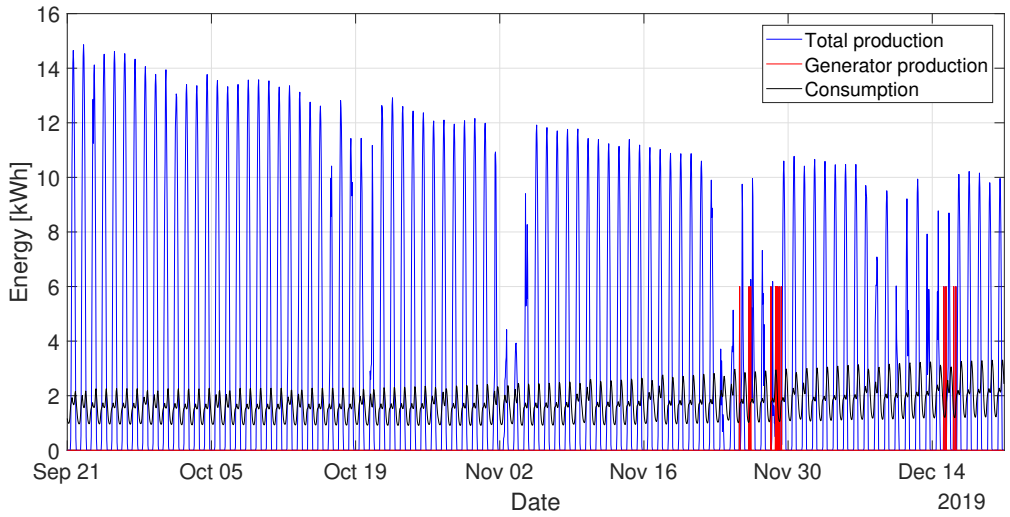

Figure 6.5: Hourly production and consumption for the Fall of 2019 with the micro CHP

In such periods, the battery level oscillated, as it can be observed in figure 6.6 and in more detail in figure 6.4, for the same reason as in the Winter. The generator produces 6 kWh per hour, and after meeting the energy needs of the building, the surplus was used to feed the batteries.

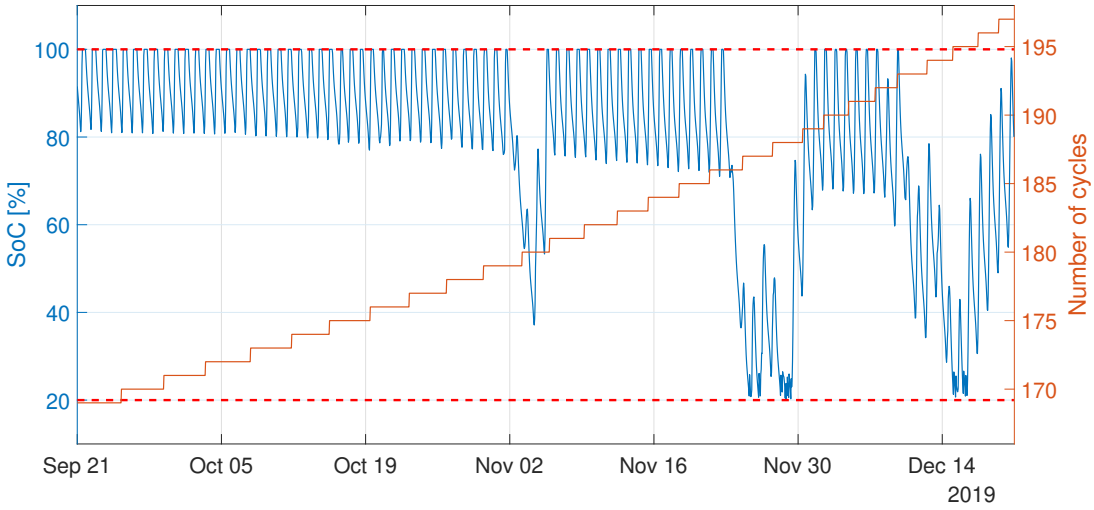

Figure 6.6: Hourly battery's SOC and cycle count for Fall 2019 with the micro CHP

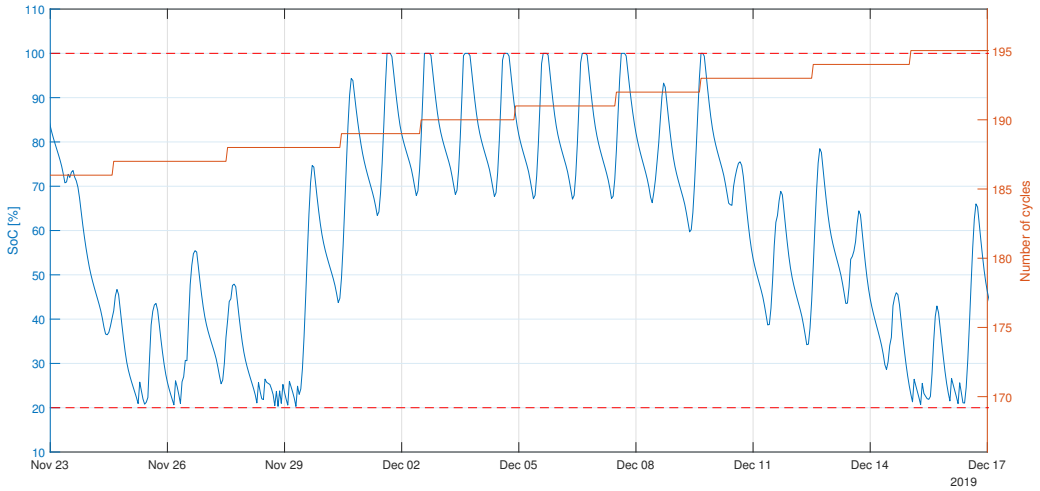

Figure 6.7: Hourly battery's SOC and cycle count for a period in the Fall of 2019 with the micro CHP

Remembering data from figures 5.8 and 5.20 , the periods where the generator was turned on, match with periods of low production, this is due to the occurrence of clouds in the sky, thus low irradiation, or due to night time. When there is the occurrence of a cloudy sky several days in a row, the system tends to require the use of an emergency source to satisfy the consumption of the building, as we observe it occurring in this case, with the micro CHP.

In the end of this analysis, it is possible to observe, in figure 6.6, that the batteries count 197 cycles, instead of 195 as observed in section 5.5.1.

6.2.2 Critical days

The only critical day where a difference on the production profile is noted, is the cloudiest day of Winter, observed in figure 5.26, this happens because on this day, as was observed in figure 5.26, the

batteries' SOC, reaches 20%, thus a deficit of energy occurs. Now with the micro CHP, it is possible to observe the alteration in production due to the emergency trigger of this device. Note in figure 6.8 that when the SOC of the batteries reaches 20%, the production increases abruptly to 6 kWh at 21:00, this is because the generator was turned on during this hour. At the end of the day, the batteries have a SOC at 20.2 %, thus, the generator is not yet turned on, but it will be turned on at midnight of the following day.

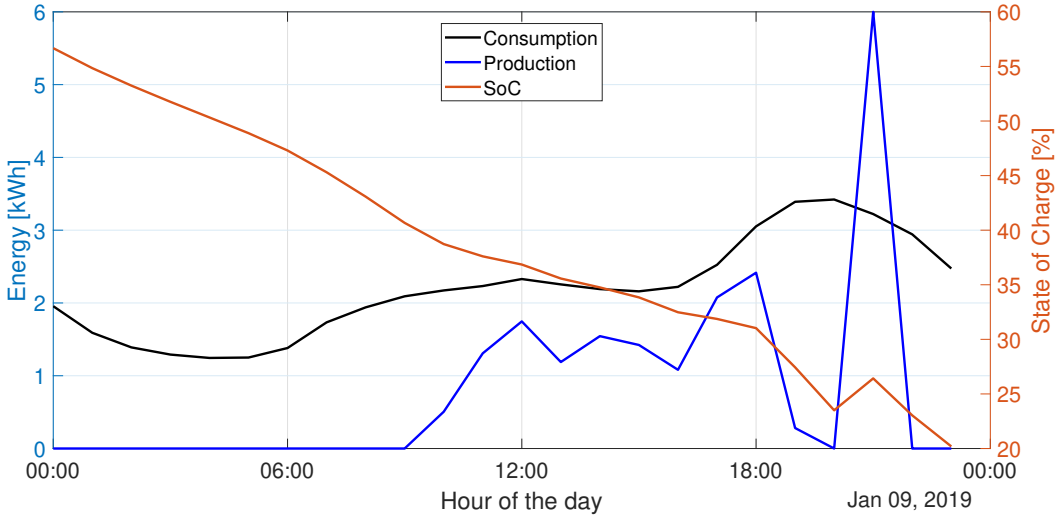

Figure 6.8: Hourly energy production, consumption and battery's SOC for the cloudiest day of Winter with the micro CHP

Chapter 7

Economic assessment

Now that the energy system can fully satisfy the energy consumption of the building, an economic assessment of such system was performed. The investment costs of the energy system are described in table 7.1. It is important to find a measure to compare the cost of the obtained system with the prices practiced by utility companies in the Portuguese market. The method used in this chapter will be focused on computing the Levelized Cost of Energy ($LCOE$) as a measure for comparison.

Investment Costs			
Devices	Price per unit [€/unit]	Units	Total [€]
PV panels	202.40	72	14 572.80
Inverter	2 020.00	6	12 120.00
MPPT	602.00	9	5 418.00
Batteries	4 686.00	9	42 174.00
XRGI	19 950.00	1	19 950.00
Storage vessel	1 100.00	1	1 100.00
Power correction factor	995.00	1	995.00
Total PV			74 284.80
Total CHP			22 045.00
Total			96 329.80

Table 7.1: Investment costs of the energy system

The $LCOE$ is the cost of energy in €/kWh, it represents the net present value of the unitary cost of electrical energy over the lifetime of a system. It is obtained by summing all the costs of a system during its lifetime, these costs include investment costs, operation and maintenance costs and fuel costs, then, this result is divided by the total electrical energy generated, this is described in equation 7.1,

$$LCOE = \frac{I_t + \sum_{j=1}^{n}[\frac{c_{om,j}}{(1+a)^j}] + \sum_{j=1}^{n}[\frac{c_{fuel,j}}{(1+a)^j}]}{\sum_{j=1}^{n}[\frac{E_j}{(1+a)^j}]} \tag{7.1}$$

Where I_t is the total investment cost, assumed to be invested, in full, in the beginning of the project (present moment), $c_{om,j}$ is the operation and maintenance costs of year j, $c_{fuel,j}$ is the fuel costs of year j, E_j is the total energy generated in year j, n is the lifetime of the energy system which is considered as equal to 5 years and a is the discount rate, which is assumed to be equal to the inflation rate for this sector (2.2% [14]). For the scope of this thesis, the operation and maintenance costs will not be

addressed and will be assumed as equal to zero. The PV panels don't have a fuel input to generate energy, however, the micro CHP has, and this had to be considered while computing the $LCOE$. The natural gas price was obtained from one of the utility companies in Portugal, EDP, and it's 0.0621 €/kWh [15]. Table 7.2, shows the data necessary to compute the $LCOE$ and the results for the $LCOE$ of the different technologies and for the building's energy system.

System	Power [kW]	Investment [€]	Specific Investment [€/kW]	Production [kWh/year]	Natural Gas Consumption [kWh/year]	$LCOE$ [€]
PV	21.6	74 284.80	3 439.11	37 622	-	0.42
CHP	6	22 045.00	3 674.17	294	976.74	16.97
Energy System	27.6	96 329.80	3490.21	37 916	976.74	0.58

Table 7.2: $LCOE$ for the different technologies and for the energy system

As shown in equation 7.2, to obtain the natural gas consumption of the micro CHP, $Cons_{naturalgas}$, one had to consider the electricity generated, $Prod_{CHP}$, and divide by the electrical efficiency of this unit, $\eta_{Elec_{CHP}}$, from the manufacturer's data sheet in appendix A.7, 30.1%

$$Cons_{naturalgas} = \frac{Prod_{CHP}}{\eta_{Electric}} \tag{7.2}$$

The value computed for the $LCOE$ of the PV system, $LCOE_{PV}$ was 0.42 €/kWh, with the use of the micro CHP only as an emergency source, the $LCOE$ for the total energy system, $LCOE_{System}$ is 0.58 €/kWh. The CHP used as a backup generator, operates for a small number of hours every year, thus, its $LCOE$, $LCOE_{CHP}$, is higher, 16.97 €/kWh. The value paid by an EDP client with 3.45 kVA of installed power, typical in a T2 apartment, and an annual consumption of 1 681 kWh (as in LVN class C), is around 0.20 €/kWh [15]. In comparison, $LCOE_{System}$ is very high, more than double. Thus, in this analysis an investment in an energy system, like the one in study, when constructing a building, is not a viable one. However, this analysis was performed considering a 5 year lifetime for the system, and a PV system usually have a lifetime of at least 20 years. Also, the $LCOE_{System}$ can be optimized in order to increase the production of the micro CHP (decreasing the $LCOE_{CHP}$) and decrease the number of batteries, which is the most expensive device of the PV system (thus, decreasing the $LCOE_{PV}$).

7.1 Sensitivity analysis

The variation of the $LCOE_{System}$ is important to assess in order to obtain a more viable solution.

The largest portion of the investment costs in the PV system is the investment cost of the batteries. Thus, the value of the $LCOE_{PV}$ is expected to vary with the number of batteries. Several values for $LCOE_{PV}$ were obtained in table 7.3.

Number of Batteries	Cost of Batteries [€]	Investment PV [€]	Specific Investment PV [€/kW]	$LCOE_{PV}$ [€/kWh]
1	4 686.00	36 796.80	1 703.56	0.21
2	9 372.00	41 482.80	1 920.50	0.24
3	14 058.00	46 168.80	2 137.44	0.26
4	18 744.00	50 854.80	2 354.39	0.29
5	23 430.00	55 540.80	2 571.33	0.32
6	28 116.00	60 226.80	2 788.28	0.34
7	32 802.00	64 912.80	3 005.22	0.37
8	37 488.00	69 598.80	3 222.17	0.39
9	42 174.00	74 284.80	3 439.11	0.42

Table 7.3: Variation of $LCOE_{PV}$ with the number of batteries

Figure 7.1 shows how the $LCOE_{PV}$ varies with the number of batteries, a decrease in the number of batteries represents a decrease in the $LCOE_{PV}$ of the system.

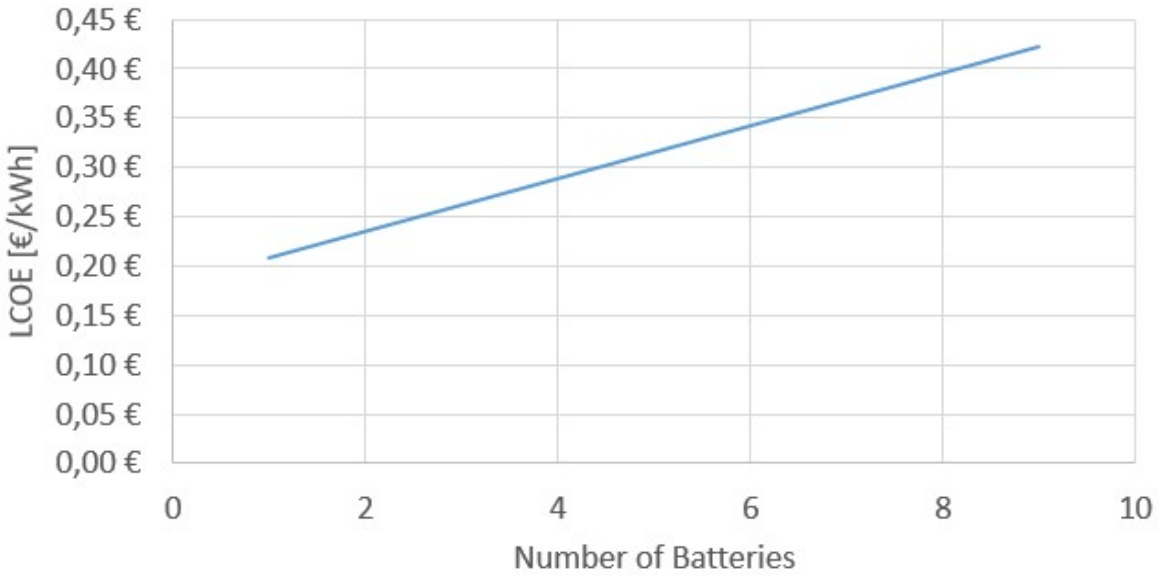

Figure 7.1: Variation of the $LCOE_{PV}$ with the number of batteries

The $LCOE_{CHP}$ varies with the amount of energy generated, if the micro CHP generates more electric energy in the same time-span, the $LCOE_{CHP}$ decreases. As the $LCOE_{CHP}$ varies with the energy generated, the investment in this this case is constant and equal to 22 045.00 €. Several values for the $LCOE_{CHP}$ were computed in table 7.4, in this table, the energy generated was computed as a function of the number of batteries. Figure 7.2 shows how the $LCOE_{CHP}$ varies with the energy produced by the micro CHP, an increase in production reflects a decrease of the $LCOE_{CHP}$.

Number of Batteries	Energy Generated by the micro CHP [kWh]	$LCOE_{CHP}$ [€/kWh]
1	5652	1.80
2	2790	2.65
3	1380	4.38
4	720	7.50
5	498	10.41
6	414	12.33
7	366	13.82
8	330	15.22
9	294	16.97

Table 7.4: Variation of the $LCOE_{CHP}$ with the number of batteries

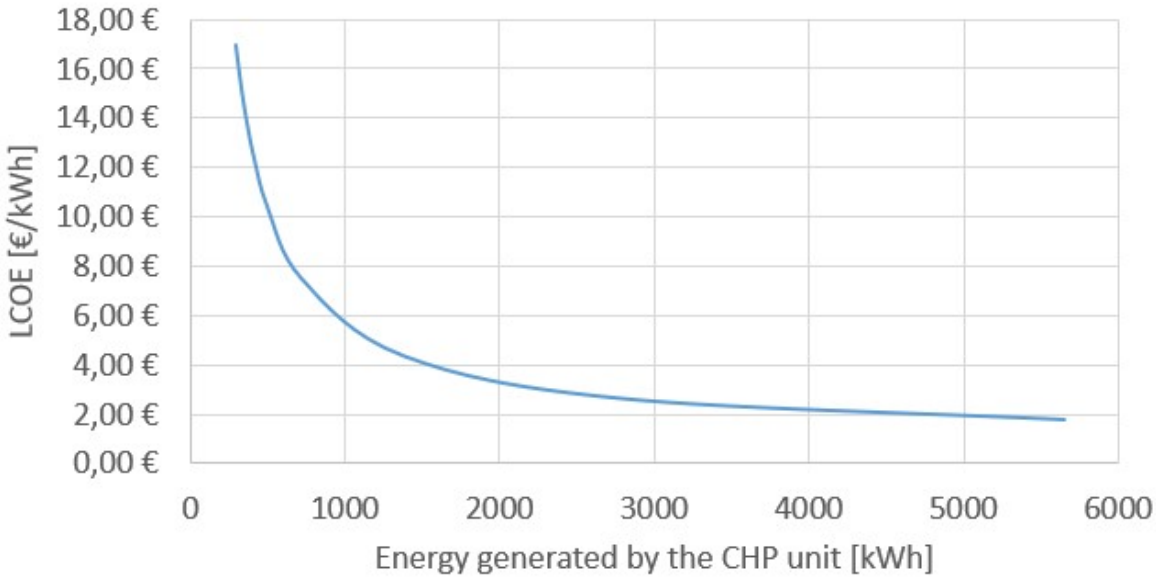

Figure 7.2: Variation of $LCOE_{CHP}$ with the amount of energy generated

For the energy system obtained by combining the two technologies, it is important to understand that a reduction in the number of batteries reflect an increase in the amount of energy produced by the micro CHP. This happens because the micro CHP works only as an emergency source, if the number of batteries is lower, there will be higher energy needs that the micro CHP has to satisfy. An optimal value can be obtained by decreasing the number of batteries and, consequently, increasing the micro CHP generation. In table 7.5 several values for the $LCOE_{System}$, were computed.

Number of Batteries	Total Investment [€]	Specific Investment [€/kW]	Production [kWh/year]	$LCOE_{System}$ [€/kWh]
1	58 841.80	2 131.95	43274	0.87
2	63 572.80	2 301.73	40412	0.64
3	68 213.80	2 471.51	39002	0.53
4	72 899.80	2 641.30	38342	0.49
5	77 585.80	2 811.08	38120	0.49
6	82 271.80	2 980.86	38036	0.51
7	86 957.80	3 150.64	37988	0.53
8	91 643.80	3 320.43	37952	0.55
9	96 329.80	3 490.21	37916	0.58

Table 7.5: Variation of the $LCOE_{System}$ with the number of batteries

Figure 7.3 shows the variation of the $LCOE_{System}$ with the number of batteries, in this figure it is possible to observe that the $LCOE_{System}$ has an optimal value.

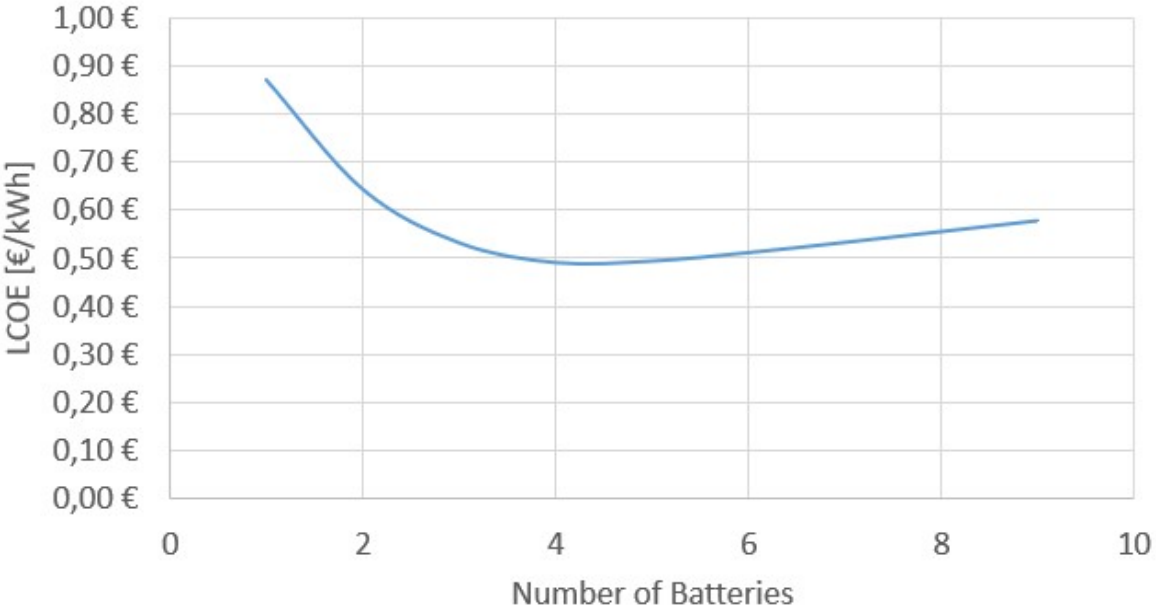

Figure 7.3: Variation of the $LCOE_{System}$ with the number of batteries

Table 7.6 shows all the values obtained for the $LCOE$ normalized, these values are compared in figure 7.4, that describes the variation of all the normalized $LCOE$ with the number of batteries. It is possible to observe that the minimum $LCOE_{System}$ is not the same as the point (with one battery) that has the minimum $LCOE$ for the technologies separately. From table 7.5 and figure 7.3, the optimal minimum value for the $LCOE_{System}$ is 0.49 €/kWh, and the system is considered to have 4 or 5 batteries.

Although this is lower than the one obtained for the system with nine batteries, it is still higher than the one used by EDP, thus, the investment is not viable.

Number of Batteries	$LCOE_{PV}$	$LCOE_{CHP}$	$LCOE_{System}$
1	10.60%	49.53%	100.00%
2	15.64%	55.84%	73.76%
3	25.79%	62.15%	60.91%
4	44.20%	68.46%	56.17%
5	61.37%	74.77%	56.63%
6	72.67%	81.08%	58.55%
7	81.45%	87.38%	61.00%
8	89.71%	93.69%	63.60%
9	100.00%	100.00%	66.20%

Table 7.6: Variation of all $LCOE$ with the number of batteries (nomalized values)

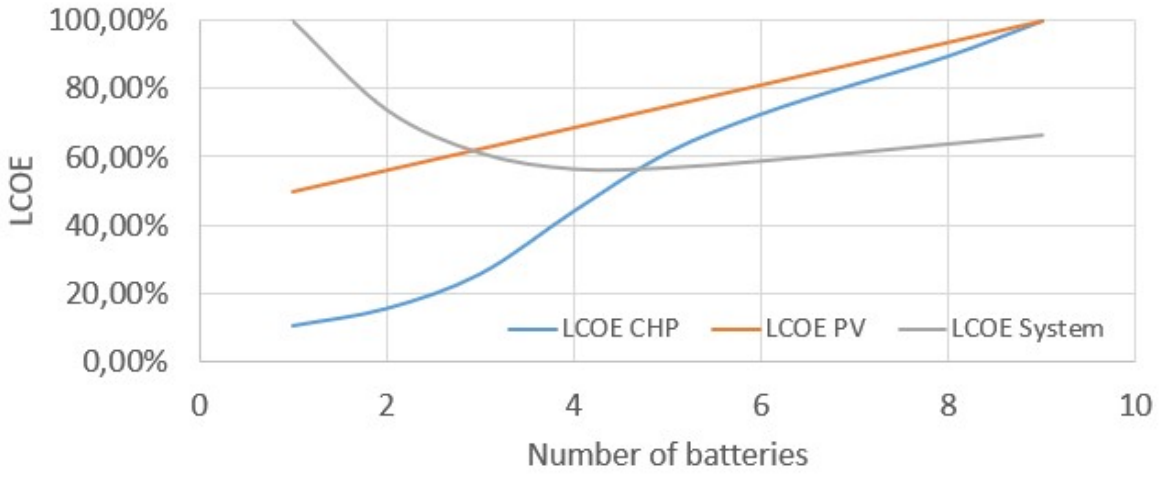

Figure 7.4: Normalized variation of all $LCOE$ with the number of batteries

Chapter 8

Conclusions

The initial PV system was analyzed and its operation and topology were defined. The power cables of the system were considered in order to obtain the power losses in cables.

A new and more suitable consumption profile was obtained, and with this, the re-sizing of the PV system was required. The PV system was re-sized considering the use of batteries. The power losses were, once again, assessed in the new PV system and they proved to be small enough to neglect. The surplus and deficit of energy without batteries was computed and it was observed that the system could store energy to meet the building's energy needs. Batteries were then implemented in the system and the system's performance was analyzed. It was observed that the designed system was not yet enough to satisfy the energy consumption of the building for the entire year. There were short periods of a few hours where the system could not satisfy the building's energy needs, mainly due to high cloud coverage of the sky. Thus, a micro CHP was implemented to work as an emergency source of energy, as a result, the energy needs of the building were satisfied. An economical analysis for the final system was performed and the system proved to be an unreliable investment compared to utility prices. A sensitivity analysis was then performed to assess the possibility of a cheaper system with less batteries, but the reduction in costs was not enough to turn this investment in a viable one.

The values of $LCOE$ obtained by Ladeira in his full roof coverage scenarios (around 120 panels), are 0.50 €/kWh and 0.34 €/kWh. These values were obtained because of several factors. The battery investment is very low compared with market prices, the investment costs do not consider the cost of auxiliary devices and the higher consumption profile has a consequence in $LCOE$ decrease. The values for $LCOE$ in the new designed system (0.58 €/kWh and 0.49 €/kWh) take in consideration a new consumption profile, auxiliary devices required and the market price for batteries.

8.1 Future Work

Energy systems for independent buildings are very important to study, the scope of this thesis is a very small beginning for what can be achieved in the energy sector in order to change the paradigm. The focus of future work can be divided in reviewing and improving this work or continuing the work done.

The PV system can be improved, it is recommended to research on more efficient and cheaper panels in the market. The assembly and operational design of the system can be rethought as well. All the devices in use can be analyzed to increase the performance of the PV system, achieving lower costs. As this is the most important source of energy of the build, it should be the focus of any reassessment of the energy system. The batteries included in the PV system can be reassessed as well, a safer battery chemistry can be found, but compatibility with the system must be ensured.

In the computational method, better real case results can be provided. The battery's self-discharge rate and the loss of capacity with the increasing cycle life were not considered. Computations using the power curve of the devices can be implemented.

The energy generated by PV panels in the Spring and Summer season is very high, and there is a lot of excess energy generated that can't be stored, it would be interesting to find a way to use all the generated energy.

The micro CHP could be more efficient for the energy system of the building if the use of heat was considered. The electricity demand in heating devices, such as boilers and heat exchangers, would decrease and more electric energy could be stored in emergency situations, as a consequence, this would decrease the use of the micro CHP.

For the economical analysis, improvements can be made by considering operation and maintenance costs for both the PV system and micro CHP, by considering the entire lifetime of the generation systems and by considering a reinvestment in batteries, if necessary.

Regarding a topic development for this work, it is possible, and should be considered, a variety of consumption profiles based on the average profile. The apartments should not have the same load. The load can be varied as a percentage of the average consumption profile. In this situation, the batteries' SOC in each floor would not be the same. An optimization tool that analyzes the energy needs of each floor and balances the stored energy between the batteries can be developed. This proposal aims to analyze an environment as close as possible to a real and more practical situation.

Bibliography

[1] Eurostat. *Energy, transport and environment indicators*. European Union, 2018.

[2] Soares, S., Alves, M., and Fragoso, R. Energy efficiency trends and policies in portugal. Technical report, Adene: Agencia para a Energia, July 2018.

[3] Eurostat. *Renewable energy statistics*. European Union, 2019.

[4] Ladeira, R. Modelling and optimisation of stationary multi-source autonomous energy supplies/storage for small buildings. Master's thesis, Grenoble INP - Ense3, 2018.

[5] Khadka, N. Solar micro grid case-studies for three electrification project sites in nepal. Master's thesis, Instituto Superior Técnico - Universidade de Lisboa, 2017.

[6] Green, M. A., Emery, K., Hishikawa, Y., Warta, W., and Dunlop, E. D. Solar cell efficiency tables (version 45). *Progress in photovoltaics: research and applications*, 2014.

[7] Carriço, J. F. E. Technical and economic assessment of a 500w autonomous photovoltaic system with lifepo4 battery storage. Master's thesis, Instituto Superior Técnico - Universidade de Lisboa, 2015.

[8] Agency, I. E. Technology roadmap solar photovoltaic energy. Technical report, IEA, 2014.

[9] Rodriguez, M. V. Sistema autónomo fotovoltaico-diesel para microprodução de energia elétrica com armazenamento de energia em baterias. Master's thesis, Instituto Superior Técnico - Universidade de Lisboa, 2017.

[10] Steven Hegedus (editor), A. L. *Handbook of Photovoltaic Science and Engineering*. John Wiley & Sons Ltd, 2003.

[11] Distribuição, E. Atualização dos perfis de consumo, de produção e de autoconsumo para o ano de 2019 documento metodológico. Technical report, EDP, January 2019.

[12] Guia técnico das classes de reação ao fogo dos cabos elétricos para instalações elétricas de baixa tensão. Technical report, Direção Geral de Energia e Geologia, Junho 2017. Versão 1.2.

[13] Cabelte. Especificação de produto: Nota cpr v1. Technical report, Cabelte, S.A., Maio 2016.

[14] PORDATA, B. d. D. d. P. C. Taxa de inflação (taxa de variação do Índice de preços no consumidor): total e por consumo individual por objectivo, October 2019. URL https://www.pordata.pt/Portugal/Taxa+de+Infla%c3%a7%c3%a3o+(Taxa+de+Varia%c3%a7%c3%a3o+do+%c3%8dndice+de+Pre%c3%a7os+no+Consumidor)+total+e+por+consumo+individual+por+objectivo-2315-181660.

[15] EDP. Tarifários, October 2019. URL https://www.edp.pt/particulares/energia/tarifarios/?prod=15391.

Appendix A

Technical Datasheets

A.1 PV panel datasheet

LG MonoX® Plus

Mechanical Properties

Cells	6 x 10
Cell Vendor	LG
Cell Type	Monocrystalline / P-type
Cell Dimensions	161.7 x 161.7 mm
# of Busbar	4
Dimensions (L x W x H)	1.686 x 1.016 x 40 mm
Static Load	6.000Pa (snow load)
	5.400Pa (wind load)
Weight	18.0 kg
Connector Type	MC4, JM601A
Junction Box	IP68 with 3 Bypass Diodes
Length of Cables	2 x 1.000 mm
Glass	High Transmission Tempered Glass
Frame	Anodized Aluminium

Certifications and Warranty

Certifications	IEC 61215, IEC 61730-1/-2
	IEC TS 62804-1 (PID)
	IEC 61701 (Salt mist corrosion test)
	IEC 62716 (Ammonia corrosion test)
	ISO 9001
Module Fire Performance	Class C, Fire Class 1 (Italy)[2]
Product Warranty	12 Years
Output Warranty of Pmax (Measurement Tolerance ±3%)	Linear Warranty[3]

[2] In progress

[3] 1) 1st year : 98% 2) after 2nd year : 0.55%p annual degradation 3) 84.8% for 25 years

Temperature Characteristics

NOCT	[°C]	45 ± 3
Pmax	[%/°C]	-0.41
Voc	[%/°C]	-0.30
Isc	[%/°C]	0.03

Characteristic Curves

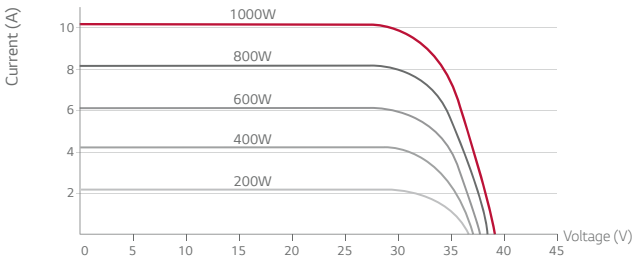

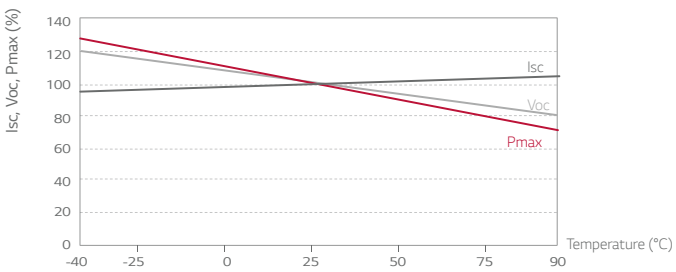

Electrical Properties (STC[4])

Model		LG300S1C-A5	LG295S1C-A5	LG290S1C-A5
Maximum Power (Pmax)	[W]	300	295	290
MPP Voltage (Vmpp)	[V]	31.7	31.3	31.0
MPP Current (Impp)	[A]	9.47	9.43	9.36
Open Circuit Voltage (Voc)	[V]	38.9	38.6	38.3
Short Circuit Current (Isc)	[A]	10.07	10.02	9.97
Module Efficiency	[%]	17.5	17.2	16.9
Operating Temperature	[°C]	-40 ~ +90		
Maximum System Voltage	[V]	1.000		
Maximum Series Fuse Rating	[A]	20		
Power Tolerance	[%]	0 ~ +3		

[4] 1) STC (Standard Test Condition): Irradiance 1000 W/m2, module temperature 25 °C, AM 1.5.
2) The typical change in module effi ciency at 200 W/m2 in relation to 1000 W/m2 is -4.5%.
3) Application Class: A, Safety Class: II
4) The nameplate power output is measured and determined by LG Electronics at its sole and absolute discretion.

Electrical Properties (NOCT[5])

Model		LG300S1C-A5	LG295S1C-A5	LG290S1C-A5
Maximum Power (Pmax)	[W]	220	216	212
MPP Voltage (Vmpp)	[V]	29.1	28.7	28.4
MPP Current (Impp)	[A]	7.56	7.53	7.47
Open Circuit Voltage (Voc)	[V]	36.0	35.7	35.4
Short Circuit Current (Isc)	[A]	8.10	8.06	8.02

[5] NOCT (Nominal Operating Cell Temperature): Irradiance 800 W/m², ambient temperature 20°C, wind speed 1 m/s

Dimensions (mm)

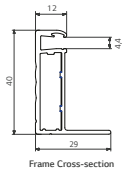

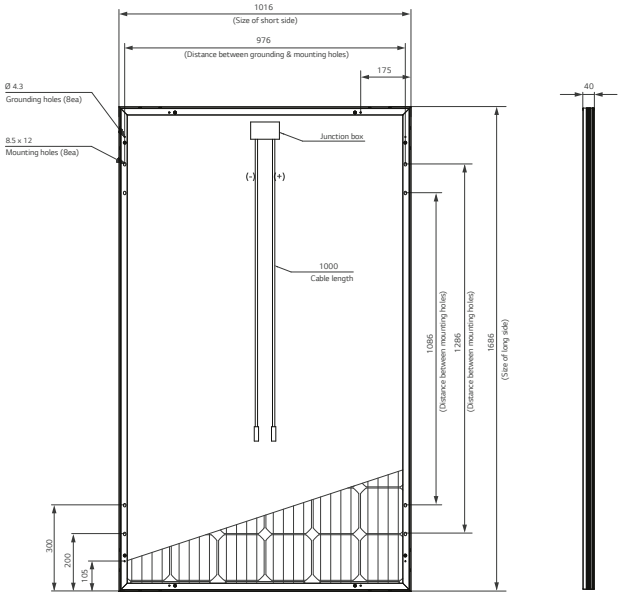

* The distance between the center of the mounting/grounding holes.

LG Electronics Deutschland GmbH
EU Solar Business Group
Alfred-Herrhausen-Allee 3–5
65760 Eschborn, Germany
E-Mail: solar@lge.de
www.lg-solar.com/uk

All details in this data sheet comply with DIN EN 50380.
Subject to errors and alterations.
Date: 01/2016
Document: DS-S1C-A5-EN-201701

A.2 Three-phase inverter datasheet

ABB string inverters

TRIO-20.0/27.6-TL-OUTD

20 to 27.6 kW

Technical data and types

Type code	TRIO-20.0-TL-OUTD	TRIO-27.6-TL-OUTD
Input side		
Absolute maximum DC input voltage ($V_{max,abs}$)	1000 V	
Start-up DC input voltage (V_{start})	430 V (adj. 250...500 V)	
Operating DC input voltage range (V_{dcmin}...V_{dcmax})	0.7 x V_{start}...950 V (min 200 V)	
Rated DC input voltage (V_{dcr})	620 V	
Rated DC input power (P_{dcr})	20750 W	28600 W
Number of independent MPPT	2	
Maximum DC input power for each MPPT ($P_{MPPTmax}$)	12000 W	16000 W
DC input voltage range with parallel configuration of MPPT at P_{acr}	440...800 V	500...800 V
DC power limitation with parallel configuration of MPPT	Linear derating from max to null [800 V≤V_{MPPT}≤950 V]	
DC power limitation for each MPPT with independent configuration of MPPT at P_{acr}, max unbalance example	12000 W [480 V≤V_{MPPT}≤800 V] the other channel: P_{dcr}-12000 W [350 V≤V_{MPPT}≤800 V]	16000 W [500 V≤V_{MPPT}≤800 V] the other channel: P_{dcr}-16000 W [400 V≤V_{MPPT}≤800 V]
Maximum DC input current (I_{dcmax}) / for each MPPT ($I_{MPPTmax}$)	50.0 A / 25.0 A	64.0 A / 32.0 A
Maximum input short circuit current for each MPPT	30.0 A	40.0 A
Number of DC input pairs for each MPPT	1 (4 in -S2X, -S2F, -S1J, -S2J versions)	1 (5 in -S2X and -S2F versions, 4 in -S1J and -S2J)
DC connection type	PV quick fit connector [3] / Screw terminal block on Standard and -S2 versions	
Input protection		
Reverse polarity protection	Yes, from limited current source	
Input over voltage protection for each MPPT - varistor	Yes, 4	
Input over voltage protection for each MPPT - plug In modular surge arrester (-S2X, -S1J and -S2J versions)	-S2X: Type 2; -S1J, -S1J: Type 1+2	
Photovoltaic array isolation control	According to local standard	
DC switch rating for each MPPT (version with DC switch)	40 A / 1000 V	
Fuse rating (versions with fuses)	15 A / 1000 V	
Output side		
AC grid connection type	Three-phase 3W+PE or 4W+PE	
Rated AC power (P_{acr} @cosϕ=1)	20000 W	27600 W
Maximum AC output power (P_{acmax} @cosϕ=1)	22000 W [4]	30000 W [5]
Maximum apparent power (S_{max})	22200 VA [6]	30670 VA [6]
Rated AC grid voltage ($V_{ac,r}$)	400 V	
AC voltage range	320...480 V [1]	
Maximum AC output current ($I_{ac,max}$)	33.0 A	45.0 A
Contributory fault current	35.0 A	46.0 A
Rated output frequency (f_r)	50 Hz / 60 Hz	
Output frequency range (f_{min}...f_{max})	47...53 Hz / 57...63 Hz [2]	
Nominal power factor and adjustable range	> 0.995, adj. ± 0.9 with P_{acr} =20.0 kW, ± 0.8 with max 22.2 kVA	> 0.995, adj. ± 0.9 with P_{acr} =27.6 kW, ± 0.8 with max 30 kVA
Total current harmonic distortion	< 3%	
AC connection type	Screw terminal block, cable gland PG36	
Output protection		
Anti-islanding protection	According to local standard	
Maximum external AC overcurrent protection	50.0 A	63.0 A
Output overvoltage protection - varistor	4	
Output overvoltage protection - plug in modular surge arrester (-S2X version)	4 (Type 2)	
Operating performance		
Maximum efficiency (η_{max})	98.2%	
Weighted efficiency (EURO/CEC)	98.0% / 98.0%	
Feed in power threshold	40 W	
Night consumption	< 0.6 W	
Communication		
Wired local monitoring	PVI-USB-RS232_485 (opt.)	
Remote monitoring	VSN300 Wifi Logger Card (opt.), VSN700 Data Logger (opt.)	
Wireless local monitoring	VSN300 Wifi Logger Card (opt.)	
User interface	Graphic display	

ABB TRIO-20.0/27.6-TL-OUTD string inverter block diagram

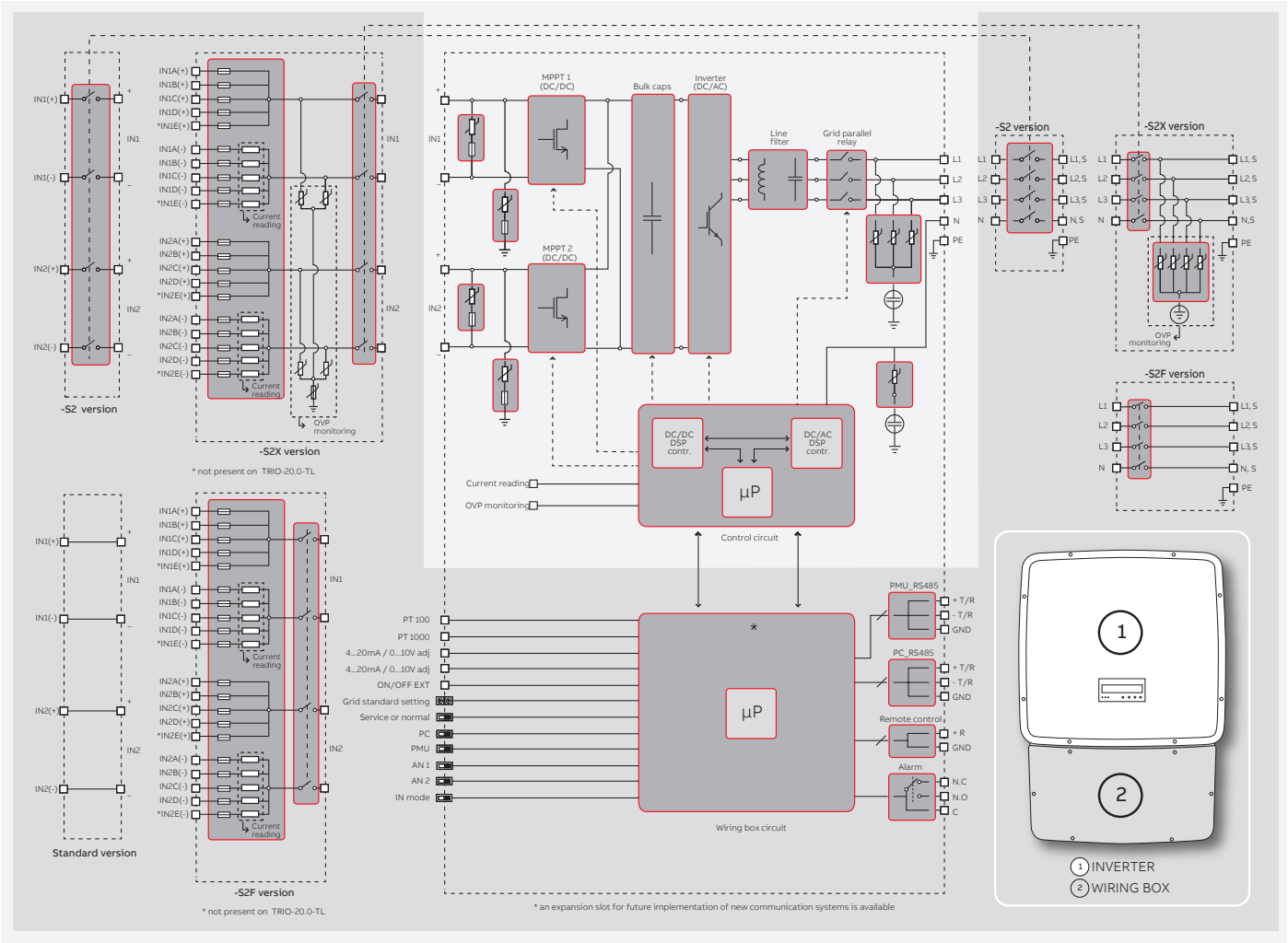

—

Technical data and types

Type code	TRIO-20.0-TL-OUTD	TRIO-27.6-TL-OUTD
Environmental		
Ambient temperature range	-25...+60°C /-13...140°F with derating above 45°C/113°F	
Relative humidity	0...100% condensing	
Sound pressure level, typical	50 dBA @ 1 m	
Maximum operating altitude without derating	2000 m / 6560 ft	
Physical		
Environmental protection rating	IP65	
Cooling	Natural	
Dimension (H x W x D)	1061 mm x 702 mm x 292 mm / 41.7" x 27.6" x 11.5"	
Weight	< 70.0 kg / 154.3 lbs (Standard version)	< 75.0 kg / 165.4 lbs (Standard version)
Mounting system	Wall bracket	
Safety		
Isolation level	Transformerless	
Marking	CE (50 Hz only), RCM	
Safety and EMC standard	EN 50178, IEC/EN 62109-1, IEC/EN 62109-2, AS/NZS 3100, AS/NZS 60950.1, EN 61000-6-2, EN 61000-6-3, EN 61000-3-11, EN 61000-3-12	
Grid standard (check your sales channel for availability)	CEI 0-21, CEI 0-16, DIN V VDE V 0126-1-1, VDE-AR-N 4105, G59/3, C10/11, EN 50438 (not for all national appendices), RD 1699, RD 413, RD 661, P.O. 12.3, AS 4777, BDEW, NRS-097-2-1, MEA, IEC 61727, IEC 62116, Ordinul 30/2013, VFR 2014	
Available products variants		
Standard	TRIO-20.0-TL-OUTD-400	TRIO-27.6-TL-OUTD-400
With DC+AC switch	TRIO-20.0-TL-OUTD-S2-400	TRIO-27.6-TL-OUTD-S2-400
With DC+AC switch and fuse	TRIO-20.0-TL-OUTD-S2F-400	TRIO-27.6-TL-OUTD-S2F-400
With DC+AC switch, fuse and surge arrester	TRIO-20.0-TL-OUTD-S2X-400	TRIO-27.6-TL-OUTD-S2X-400
With DC+AC switch, fuse and 1 DC surge arrester Type 1 + 2	TRIO-20.0-TL-OUTD-S1J-400	TRIO-27.6-TL-OUTD-S1J-400
With DC+AC switch, fuse and 2 DC surge arrester Type 1 + 2	TRIO-20.0-TL-OUTD-S2J-400	TRIO-27.6-TL-OUTD-S2J-400

[1] The AC voltage range may vary depending on specific country grid standard
[2] The Frequency range may vary depending on specific country grid standard
[3] Please refer to the document "String inverters – Product manual appendix" available at www.abb.com/solarinverters for information on the quick-fit connector brand and model used in the inverter

[4] Limited to 20000 W according to country specific regulations
[5] Limited to 27600 W according to country specific regulations
[6] Due to country specific regulations this value can be limited to 22000VA/30000VA
Remark. Features not specifically listed in the present data sheet are not included in the product

Efficiency curves of TRIO-20.0-TL-OUTD

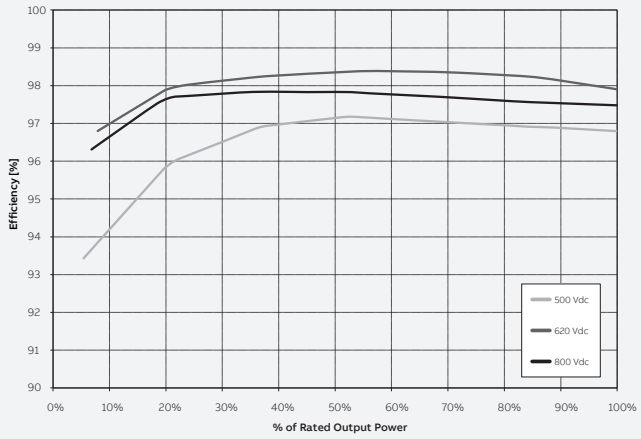

Efficiency curves of TRIO-27.6-TL-OUTD

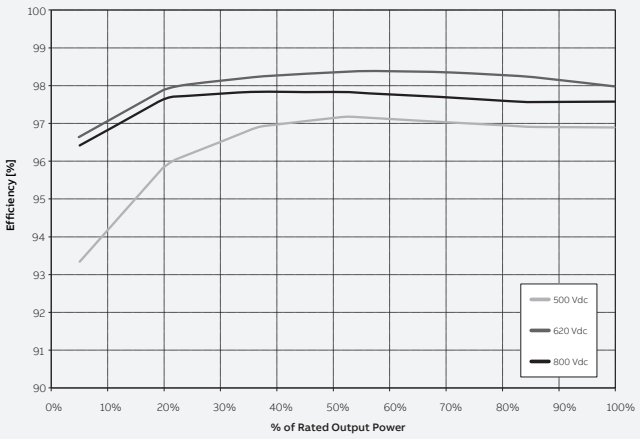

For more information please contact your local ABB representative or visit:

www.abb.com/solarinverters
www.abb.com

BCD.00379_EN REV L 05.02.2019

A.3 Power cables table

CARACTERÍSTICAS DIMENSIONAIS E ELÉCTRICAS

Composição do cabo nº. cond.x secção (mm^2)	Diâmetro exterior aprox. (mm)	Peso aprox. (kg/km)	Corrente máxima admissível (A) Ta=30°C Instalação em tubos embebidos nos elementos da construção, em alvenaria	
			2 condutores carregados	3 condutores carregados
		H07V-U		
1 x 1,5	3,0	20	17,5	15,5
1 x 2,5	3,5	30	24	21
1 x 4	4,0	45	32	28
1 x 6	4,5	65	41	36
		H07V-R		
1 x 1,5	3,5	20	17,5	15,5
1 x 2,5	4,0	35	24	21
1 x 4	4,5	50	32	28
1 x 6	5,0	70	41	36
1 x 10	6,5	110	57	50
1 x 16	7,5	180	76	68
1 x 25	9,0	265	101	89
1 x 35	10,0	350	125	110
1 x 50	11,5	490	151	134
1 x 70	13,5	695	192	171
1 x 95	15,5	960	232	207
1 x 120	17,0	1200	269	239
1 x 150	19,0	1450		
1 x 185	21,0	1845		
1 x 240	24,0	2405		
1 x 300	26,5	3045		
1 x 400	30,0	3845		
		H07V-K		
1 x 6	5,5	70	41	36
1 x 10	6,5	110	57	50
1 x 16	8,5	175	76	68
1 x 25	9,5	255	101	89
1 x 35	11,0	350	125	110
1 x 50	13,5	515	151	134
1 x 70	15,0	675	192	171
1 x 95	16,5	890	232	207
1 x 120	18,5	1145	269	239
1 x 150	20,5	1420		
1 x 185	22,5	1715		
1 x 240	29,0	2310		

1 só circuito instalado, método de referência B (RTIEBT)

A.4 Inverter charger datasheet

Xtender series

	Model	XTS 900-12	XTS 1200-24	XTS 1400-48	XTM 1500-12	XTM 2000-12	XTM 2400-24	XTM 2600-48	XTM 3500-24	XTM 4000-48	XTH 3000-12	XTH 5000-24	XTH 6000-48	XTH 8000-48
	Inverter													
	Nominal battery voltage	12Vdc	24Vdc	48Vdc	12Vdc		24Vdc	48Vdc	24Vdc	48Vdc	12Vdc	24Vdc	48Vdc	
	Input voltage range	9.5 - 17Vdc	19 - 34Vdc	38 - 68Vdc	9.5 - 17Vdc		19 - 34Vdc	38 - 68Vdc	19 - 34Vdc	38 - 68Vdc	9.5 - 17Vdc	19 - 34Vdc	38 - 68Vdc	
	Continuous power @ 25°C	650**/500VA	800**/650VA	900**/750VA	1500VA	2000VA	2000VA	2000VA	3000VA	3500VA	2500VA	4500VA	5000VA	7000VA
	Power 30 min. @ 25°C	900**/700VA	1200**/1000VA	1400**/1200VA	1500VA	2000VA	2400VA	2600VA	3500VA	4000VA	3000VA	5000VA	6000VA	8000VA
	Power 5 sec. @ 25°C	2.3kVA	2.5kVA	2.8kVA	3.4kVA	4.8kVA	6kVA	6.5kVA	9kVA	10.5kVA	7.5kVA	12kVA	15kVA	21kVA
	Maximum load	Up to short-circuit												
	Maximum asymmetric load	Up to Pcont.												
*	Load detection (stand-by)	2 to 25 W												
	Cos φ	0.1-1												
	Maximum efficiency	93%	93%	93%	93%		94%	96%	94%	96%	93%	94%	96%	
	Consumption OFF/Stand-by/ON	1.1W/1.4W/7W	1.2W/1.5W/8W	1.3W/1.6W/8W	1.2W/1.4W/8W	1.2W/1.4W/10W	1.4W/1.6W/9W	1.8W/2W/10W	1.4W/1.6W/12W	1.8W/2.1W/14W	1.2W/1.4W/14W	1.4W/1.8W/18W	1.8W/2.2W/22W	1.8W/2.4W/30W
*	Output voltage	Pure sine wave 230Vac (±2%) / 120Vac (1)												
*	Output frequency	45Hz - 60Hz (1) ± 0.05% (crystal controlled)												
	Harmonic distortion	<2%												
	Overload and short-circuit protection	Automatic disconnection with 3 time restart attempt												
	Overheat protection	Warning before shut-off - with automatic restart												
	Battery charger													
*	Charge Characteristic	6 steps: Bulk-Absorption-Floating-Equalization-reduced floating-periodic absorption Number of steps, thresholds, end current and times completely adjustable with the RCC-02/-03												
*	Maximum charging current	35A	25A	12A	70A	100A	55A	30A	90A	50A	160A	140A	100A	120A
*	Temperature compensation	With BTS-01 or BSP 500/1200												
	Power Factor Correction (PFC)	EN 61000-3-2												
	General data	**XTS 900-12**	**XTS 1200-24**	**XTS 1400-48**	**XTM 1500-12**	**XTM 2000-12**	**XTM 2400-24**	**XTM 2600-48**	**XTM 3500-24**	**XTM 4000-48**	**XTH 3000-12**	**XTH 5000-24**	**XTH 6000-48**	**XTH 8000-48**
*	Input voltage range	150 to 265Vac / 50 to 140Vac (1)												
	Input frequency	45 to 65Hz												
	Input current max. (transfer relay) / Output current max.	16Aac/20Aac			50Aac/56Aac									50Aac/80Aac
	Transfer time	<15ms												
	Multifunction contacts	Module ARM-02 with 2 contacts, in option			2 independent contacts (potential free 3 points, 16Aac/5Adc)									
	Weight	8.2 kg	9 kg	9.3 kg	15 kg	18.5 kg	16.2 kg		21.2 kg	22.9 kg	34 kg	40 kg	42 kg	46 kg
	Dimension hxwxl [mm]	110x210x310			133x322x466						230x300x500			
	Protection index	IP54			IP20									
	Conformity	Directive EMC 2004/108/EC: EN 61000-6-1, EN 61000-6-3, EN 55014, EN 55022, EN 61000-3-2, 62040-2 Low voltage directive 2006/95/EC: EN 62040-1-1, EN 50091-2, EN 60950-1												
	Operating temperature range	-20 to 55°C												
	Relative humidity in operation	100%			95% without condensation									
	Ventilation	Optional cooling module ECF-01			Forced from 55°C									
	Acoustic level	<40dB / <45dB (without/with ventilation)												
	Warranty	5 years												
	Accessoires													
	Remote control RCC-02 or RCC-03	•	•	•	•	•	•	•	•	•	•	•	•	•
	Module XCOM-232i	•	•	•	•	•	•	•	•	•	•	•	•	•
	Internet based communication sets Xcom-LAN, Xcom-GSM	•	•	•	•	•	•	•	•	•	•	•	•	•
	Remote Control Module RCM-10 (3 m)	•	•	•	•	•	•	•	•	•				
	2 aux. contacts module ARM-02	•	•	•										
	Cooling Module ECF-01	•	•	•										
	Battery temp. sensor BTS-01 (3 m)	•	•	•	•	•	•	•	•	•	•	•	•	•
	Communication cable for 3ph and // CAB-RJ45-8-2	•	•	•	•	•	•	•	•	•	•	•	•	•
	Mounting frame X-Connect										•	•	•	•

* Adjustable with the RCC-02/-03

** These features are valid only when using the cooling module ECF-01.

(1) With -01 at the end of the reference, means 120V/60Hz. Available for all Xtenders except XTH 8000-48

Data may change without any notice.

v 1.2.0

A.5 MPPT charge controller datasheet

VarioTrack Series

Model	VT-65			VT-80		
Electrical characteristics PV array side						
At nominal battery voltage	12 V	24 V	48 V	12 V	24 V	48 V
Maximum solar power recommended (@STC)	1000 W	2000 W	4000 W	1250 W	2500 W	5000 W
Maximum solar open circuit voltage	75 V	150 V		75 V	150 V	
Maximum solar functional circuit voltage	75 V	145 V		75 V	145 V	
Minimum solar functional circuit voltage	Above battery voltage					
Electrical characteristics battery side						
Maximum output current	65 A			80 A		
Nominal battery voltages	Automatic / manual set to 12, 24 or 48 V					
Operating voltage range	7 - 68 V					
Performances of the device						
Power conversion efficiency (in a 48 V typical-system)	> 99 %					
Maximum stand-by self-consumption (48 V)	25 mA > 1.2 W					
Maximum stand-by self-consumption (24 V)	30 mA > 0.8 W					
Maximum stand-by self-consumption (12 V)	35 mA > 0.5 W					
Charging stages	4 stages: Bulk, Absorption, Float, Equalization					
Battery temperature compensation (available with accessory BTS-01)	–3 mV / °C /cell (25°C ref) default value adjustable -8 to 0 mV / °C					
Electronic protections						
PV reverse polarity	Up to –150 V					
Battery reverse polarity	Up to –150 V					
Battery overvoltage	Up to 150 V					
Over temperature	Protected					
Reverse current at night	Prevented by relays					
Environment						
Operating ambient temperature range	–20 to 55°C					
Humidity	100 %					
Ingress protection of enclosures	IP54, IEC/EN 60529:2001					
Mounting location	indoor					
General data						
Warranty	5 years					
ISO Certification	9001:2008 / 14001:2004					
Weight	5.2 kg			5.5 kg		
Dimensions h/w/l [mm]	120 / 220 / 310			120 / 220 / 350		
Parallel operation (separated PV arrays)	Up to 15 devices					
Max wire size	35 mm^2					
Glands	M 20 x 1,5					
Communication						
Network cabling	STUDER communication BUS					
Remote control & Communication	RCC-02/-03, Xcom-232i / Xcom-LAN / Xcom-GSM / Xcom-SMS					
Menu languages	English / French / German / Spanish					
Data logging	With RCC-02/03, Xcom-232i on SD card · One point every minute					
Accordance to standards						
EU declaration of conformity	**Low Voltage Directive (LVD) 2014/35/EU:** - EN 50178:1997 **Electromagnetic Compliance (EMC) Directive 2014/30/EU:** - EN 61000-6-2:2005, - EN 61000-6-4:2007/A1:2011					
Accessories						
Remote control RCC-02 or RCC-03	•			•		
Module Xcom-232i	•			•		
Communication sets Xcom-LAN / Xcom-GSM / Xcom -SMS	•			•		
Battery Status Processor BSP	•			•		
2 aux. contacts module ARM-02	•			•		
Cooling Module ECF-01	•			Included		
Battery temp. sensor BTS-01 (3 m)	•			•		
Communication cable CAB-RJ45-8-2	•			•		

Data may change without any notice

A.6 Battery datasheet

PREFACE

ESS 7.0/9.0/X is a new modular lithium-ion based energy storage system, which stores the surplus of the collected solar energy for later use. Energy can either be directed into the storage system or be fed into the public grid via an inverter.

Energy is available as required: in the evening, at night, or on a cloudy day.

With the ESS 7.0/9.0/X System, consumers of solar power become more independent from electricity prices and use their home-made eco-electricity when they need it.

ADVANTAGES

- Technical service online and by telephone
- Store during the day; use day and night
- Independent from daylight and public grid
- Economic, cost-cutting and ecofriendly
- Robust, safe and space saving
- Modular installation: the storage capacity can be adapted to your needs
- Subsidized by the Federal Government of Germany: KfW-Program 275

TECHNICAL PROPERTIES

- Powerful energy storage system
- New lithium-ion technology: a 10 year warranty covering the system's current value (not in all countries)
- High efficiency: 95 %
- High discharge depth: 80 % DOD (Depth of Discharge)
- Durable: 5,000 full cycles
- Parallel installation of max. 12 modules possible
- High operational safety

SAFETY MEASURES

- Direct current relay and 2nd protection (chemical fuse) for a redundant battery cut-off
- Overvoltage and low voltage monitoring for each cell string with redundant battery cut-off
- Temperature monitoring for each cell string
- Current interrupt device (CID) in each cell
- Protection against a reboot after deep discharge or any other serious error
- Active current control as a function of cell voltage and temperature (derating)
- Closed metal, double housing

TECHNICAL PROPERTIES OF A SINGLE MODULE

GENERAL PROPERTIES	ESS 7.0	ESS 9.0	ESS X
Energy (nom./usable)	6.74 kWh/5.39 kWh	8.5 kWh/6.8 kWh	10.06 kWh/8.05 kWh
Nominal voltage	55.5 V	54.0 V	54.0 V
Charge end voltage	61.5 V	61.5 V	61.5 V
Discharge end voltage	45.0 V	45.0 V	45.0 V
Capacity (nom./usable)	121.5 Ah/ 97.2 Ah	156.6 Ah/125.3 Ah	186.3 Ah/149.1 Ah
Max. charge	90 A	90 A	90 A
Max. discharge current	300 A (3 sec)	300 A (3 sec)	300 A (3 sec)
Max. discharge power	18 kW*	18 kW*	18 kW*
Weight	95 kg	97 kg	99 kg
Dimensions (W x H x D)	638 x 421 x 487 mm	638 x 421 x 487 mm	638 x 421 x 487 mm
Communication	CAN – SMA ready	CAN – SMA ready	CAN – SMA ready
Battery chemistry	Li-Ion NMC	Li-Ion NCA	Li-Ion NCA
Discharge depth	80% DOD	80% DOD	80% DOD
Full cycles	5,000	5,000	5,000
Battery Management System	Monitoring of cell voltage, cell temperature, current, derating and passive balancing		

PERFORMANCE DATA			
Energy density (weight)	71 Wh/kg	87.6 Wh/kg	101.6 Wh/kg

ESS 7.0/9.0/X

DEVELOPED ACCORDING TO THE STANDARDS AND USER GUIDELINES FOR STATIONARY ENERGY STORAGE SYSTEMS

- VDE-AR-E 2510-50
- VDE-AR-E 2510-2
- DIN EN 62619 (draft)
- FNN note (04/2016 version)

USER INFORMATION

- Discharge temperature (cells): 2 °C to +45 °C
- Charge temperature (cells): 2 °C to +45 °C
- Recommended storage temperature: 10 °C to 25 °C
- Self discharge (cells): ca. 2 % per year
- Stand-by consumption: Active mode 5 W / Sleep mode 0.126 W
- Max. parallel connection (of batteries): 12 (additional hardware required)
- Protection class: IP 21
- European Conformity (CE): yes
- UN-test 38.3: yes
- Warranty: 10 year warranty covering the system's current value (not in all countries)

*depends on the respective inverter

A.7 CHP generator datasheet

TECHNICAL DATA FOR THE XRGI® 6

Product data sheet in accordance with Regulation (EU) No. 811/2013; 813/2013, Dated 26.09.2019

A+++

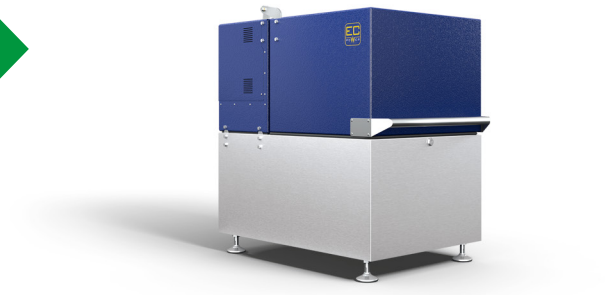

The XRGI® is a combined heat and power plant (CHP) that works on the principle of cogeneration.

An XRGI® system consists of three main components – the Power Unit, Q-Heat Distributor and the iQ-Control Panel.

In addition, you can also extend your XRGI® system with a storage tank with a capacity of 500, 800 or 1,000 litres for optimum operation.

ORDERING DATA

Supplier's name or trademark	EC POWER	
Supplier's model identifier	**XRGI® 6 without condensing technology[1]**	**XRGI® 6 with condensing technology[1]**
Article number	X060001	X060001+K000104
Modules	Power Unit, iQ10-Control Panel, Q20-Heat Distributor	Power Unit, iQ10-Control Panel, Q20-Heat Distributor + Condensing and exhaust gas heat exchanger BW4+

ErP-LABEL DATA[2]

Seasonal space heating energy efficiency class		A+++	A+++
Rated heat output	P_{rated}	12 kW	14 kW
Seasonal space heating energy efficiency; HCV[3]	η_s	**170 %**	**198 %**
Sound power level, indoors	L_{WA}	63 dB	63 dB
Electrical efficiency; in accordance with heating value LCV[3]	$\eta_{el\ CHP100+SUP\ 0}$	30 %	30 %
All special precautions to be taken during assembly, installation or service		Refer to Commissioning and Service Manual	Refer to Commissioning and Service Manual

[1] Return temperatures as per EN 50465 2015 7.6.1: Without condensing technology 47 °C, with condensing technology 30 °C.
[2] The values were rounded in accordance with the requirements governing product data sheets by Regulation (EU) No. 811/2013; 813/2013.
[3] HCV = higher calorific value, LCV = lower calorific value

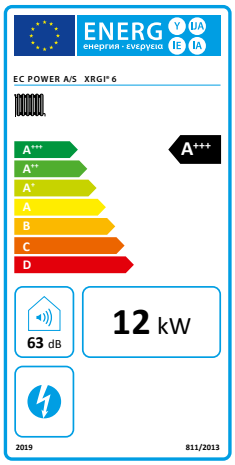

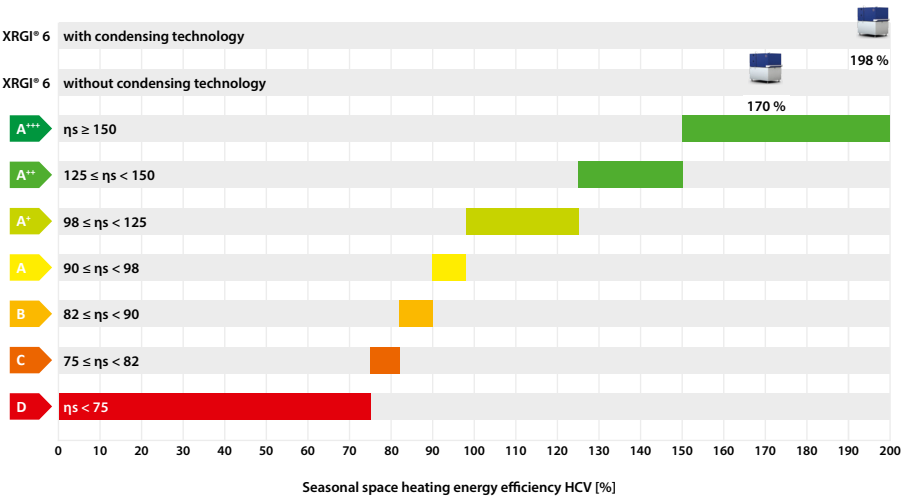

OUTPUT

XRGI® system			XRGI® 6 without condensing technology[1]			XRGI® 6 with condensing technology[1]		
Power modulation*			50 %	75 %	100 %	50 %	75 %	100 %
Electrical output, modulating*		kW	3.0	4.5	6.0	3.0	4.5	6.0
Thermal output, modulating*		kW	8.1	10.1	12.4	9.3	11.7	14.4
Power consumption, gas in accordance with LCV[2]		kW	12.0	15.7	20.0	12.0	15.7	20.0
Electrical own demand, production		kW	0.035	0.035	0.035	0.035	0.035	0.035
Electrical own demand, stand-by		kW		0.024			0.024	

EFFICIENCIES & OPERATING PARAMETERS

Power modulation*			50 %	75 %	100 %	50 %	75 %	100 %
Electrical efficiency	in accordance with LCV[2]	%	24.8	28.5	30.1	24.8	28.5	30.1
Thermal efficiency	in accordance with LCV[2]	%	67.6	64.5	62.3	77.5	74.5	72.3
Total efficiency	in accordance with LCV[2]	%	92.4	93.0	92.4	102.3	103.0	102.4
Seasonal space heating energy efficiency in operating mode[3,4]	η_{son}	%		175			202	

POWER MODULATION

Continuous modulation of 2,5 – 6 kW in power-controlled mode

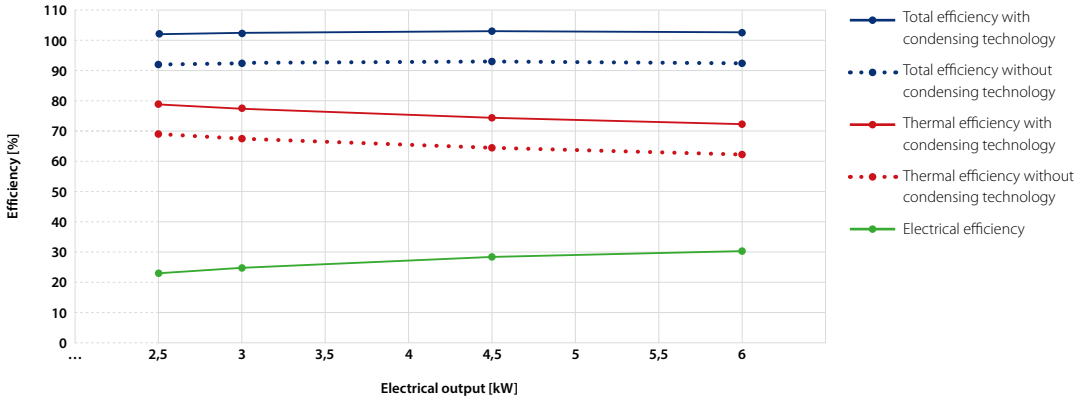

TOTAL EFFICIENCY AT FULL LOAD

XRGI® 6 total efficiency / return temperature

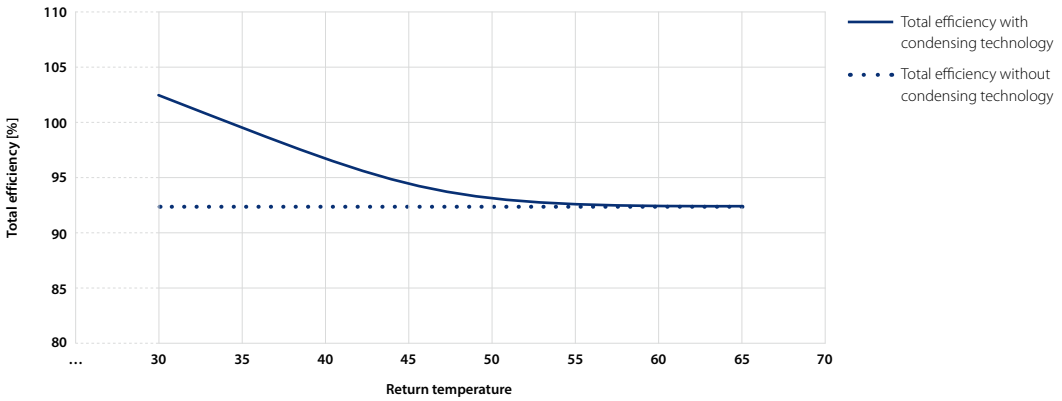

* Continuous modulation in power-controlled mode

[1] Return temperatures as per EN 50465 2015 7.6.1: Without condensing technology 47 °C, with condensing technology 30 °C.

[2] LCV = lower calorific value

[3] This values are based on independent, certified and authorised inspection bodies. Test reports are available upon request.

[4] Efficiency at rated heat output as per the delegated Commission Regulation (EU) No. 811/2013; 813/2013

HYDRAULIC INTEGRATION

Principle circuit diagram: Series circuit with injection – boiler with header

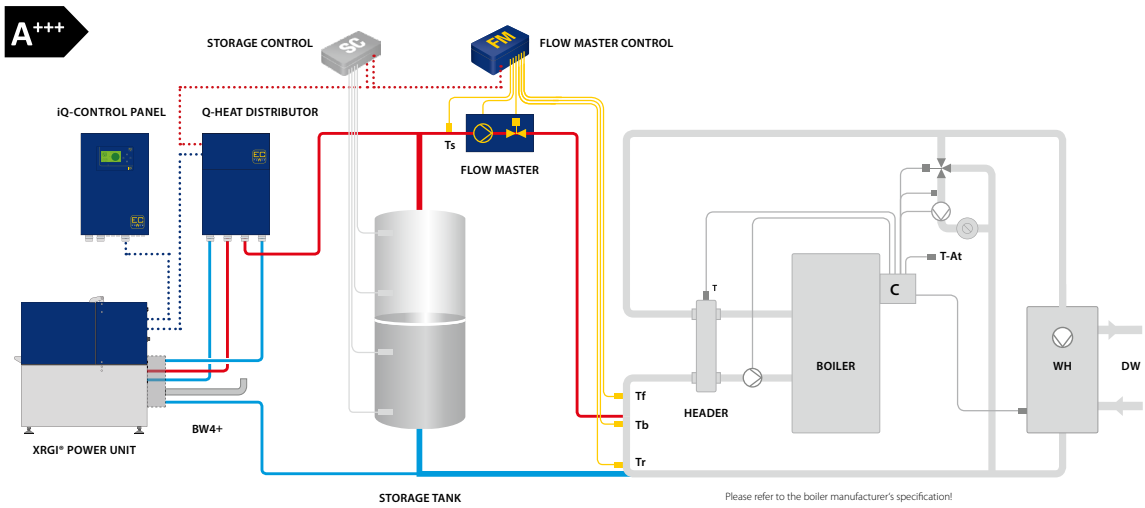

More principle circuit diagrams and information can be found in the EC POWER „Hydraulic Solutions".

NOTE:
If products from other companies are used in the system in addition to EC Power products, EC POWER assumes no liability for the accuracy of the energy efficiency class calculation for the entire system.

XRGI® system		XRGI® 6 without condensing technology[1]	XRGI® 6 with condensing technology[1]
Flow temperature, constant	°C	~ 80	~ 80
Return temperature, variable	°C	5-70	5-70

FUELS

Natural gas (all qualities), propane, butane	yes	yes

EXHAUST GAS

Power modulation*			50 %	75 %	100 %	50 %	75 %	100 %
Max. exhaust gas temperature		°C	-	-	100	-	-	90
Condensate		kg/h	-	-	-	1.4	1.8	2.1
Emissions (Test data at max. output)	CO < 150	mg/Nm³	12			13		
	NOx, pond, HCV[2,3] < 240	mg/kWh	230			217		

SOUND

Sound pressure level at a distance of up to 1 m (based on surroundings)	dB(A)	49

POWER CONNECTION

Voltage, 3 phases + N + Earth	V	400
Frequency	Hz	50

SERVICE

Service interval (operating hours)	Hours	10,000

DIMENSIONS AND WEIGHT

		XRGI® 6 Power Unit	Q20-Heat Distributor	iQ10-Control Panel
Dimensions, W x H x D	mm	640 x 960 x 930	400 x 600 x 195	400 x 600 x 210
Footprint	m²	0.59	wall mounted	wall mounted
Weight	kg	440	25	30

* Continuous modulation in power-controlled mode

[1] Return temperatures as per EN 50465 2015 7.6.1: Without condensing technology 47 °C, with condensing technology 30 °C.

[2] as per the delegated Commission Regulation (EU) No. 811/2013; 813/2013

[3] HCV = higher calorific value

Deviations in values depend on the ambient and operating conditions, tolerance +/- 5 %.
Subject to technical modifications, deviations from design and errors.